Title
CHEMILUMINESCENCE OF IF IN THE GAS PHASE REACTION OF I2 WITH F2

Authors
Birks, John W.
Gabelnick, Steven D.
Johnston, Harold S.

Publication Date
1974-12-01

Submitted to Journal of Molecular Spectroscopy

LBL-3562
Preprint

CHEMILUMINESCENCE OF IF IN THE GAS PHASE REACTION OF I_2 WITH F_2

John W. Birks, Steven D. Gabelnick, and Harold S. Johnston

December, 1974

Prepared for the U. S. Atomic Energy Commission
under Contract W-7405-ENG-48

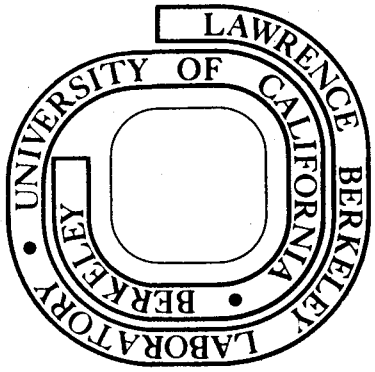

LBL-3562

DISCLAIMER

LBL-3562

Chemiluminescence of IF in the Gas Phase Reaction of I_2 with F_2

by

John W. Birks*, Steven D. Gabelnick†

and

Harold S. Johnston

Department of Chemistry and
Inorganic Materials Research Division
Lawrence Berkeley Laboratory
University of California
Berkeley, California 94720

*Present Address:
Department of Chemistry
University of Illinois at Urbana-Champaign
Urbana, Illinois 61801

†Present Address:
Chemical Engineering Division
Argonne National Laboratory
Argonne, Illinois 60439

Abstract

Emission from both the $B^3\Pi_{o+}$ state and the previously unreported $A^3\Pi_1$ state has been observed in the gas phase reaction of I_2 with F_2 at low pressures. For the $B^3\Pi_{o+}$ state the transition moment and vibrational populations were extracted from the spectra by at least squares method whereby theoretical band shapes were fit to the experimental data. The effect of flow rates of reactants and Ar on the relative emission from the two electronic states, the effect of pressure on the $B^3\Pi_{o+}$ state, and extinction of emission near 470 nm all favor the population of excited electronic states through a four-center reaction complex, rather than association of F and I atoms.

It is argued that there is an avoided curve crossing between the lowest two $^3\Pi_{o+}$ states of IF, and that the ground state dissociation energy is 23229 ± 100 cm^{-1}. The radiative lifetime of the $B^3\Pi_{o+}$ state is estimated to be 10^{-3} sec and to be much shorter than that of the $A^3\Pi$. state.

INTRODUCTION

The emission spectrum of iodine monofluoride (IF) was first reported in 1951 by Durie[1] under low resolution. The rotationally resolved spectrum was later reported by Durie[2], thus confirming the existence of this molecule which is thermodynamically unstable with respect to disproportionation to give the products I_2 and IF_5. Due to absence of a Q branch in the high resolution spectrum, the emission was assigned to the IF ($B^3\Pi_{o+} \rightarrow X^1\Sigma^+$) transition analogous to other halogen and interhalogen spectra. In both studies the source of the IF spectrum was an iodine-fluorine flame in which F_2 passed over iodine crystals.

Clyne, Coxon and Townsend[3] studied the emission resulting from the association of ground state I ($^2P_{3/2}$) atoms and F($^2P_{3/2}$, $^2P_{1/2}$) atoms in the presence of singlet oxygen ($^1\Delta g$, $^1\Sigma_g^+$). They observed many of the same bands as Durie and a number of bands at longer wavelengths that belong to the same band system.

We have studied the emission resulting from the gas phase reaction of I_2 with F_2 in a flow system at pressures as low as 4×10^{-3} torr. In addition to bands belonging to the IF($B^3\Pi_{o+} \rightarrow X^1\Sigma^+$) system, we observed bands in the same wavelength region originating in a lower-lying bound molecular state. The relative amounts of emission from the two excited electronic states varied with the flow rates of I_2 and Ar so

that spectra could be obtained in which emission occurred predominantly from either one of the two excited electronic states. We assign this previously unreported emission to the $IF(A^3\Pi \rightarrow X^1\Sigma^+)$ transition. Emission from the $A^3\Pi_1$ state for diatomic halogens and interhalogen has been reported previously for Br_2[4,5,7] I_2[7], ICl[6] and IBr[4]. We have also studied the effect of pressure on the vibrational populations of the $B^3\Pi_o^+$ state.

EXPERIMENTAL

A. Reaction cell and flow system

Figure 1 is a schematic diagram of the apparatus. The reaction cell consisted of a large stainless steel tank with a cylindrical portion 62 cm in diameter and 76 cm long and hemispherical ends. The volume of the cell was 350 liters. Preliminary experiments were carried out in a 1 liter spherical cell.[8] Pressures in the cell were measured with a factory calibrated Datametrics Type 1014 Barocel electronic manometer. Effluent gases passed over trays of NaCl heated to 100 °C to exchange F_2 for Cl_2 which was then removed by a liquid nitrogen trap. The cell was continuously pumped on by a mercury diffusion pump and an oil forepump.

Fluorine, obtained from Matheson Co. (98% purity), was passed over activated NaF to remove HF impurity and stored in a 34 liter tank at pressures less than one atmosphere. From this storage tank fluorine was metered into the reaction cell

by means of a Vactronics leak valve. Argon of 99.996% purity obtained from Linde Inc. was metered into the cell by a leak valve also and mixed with fluorine prior to entering the cell. Flow rates of fluorine and argon were measured using Hastings-Raydist Model LF-50 calorimetric mass flowmeters.

Analytical reagent grade iodine obtained from Mallincrockdt was held at 313 K in a glass bulb submerged in a constant temperature mineral oil bath. The vacuum line and valves connecting the bulb to the cell were heated to prevent sublimation. Due to the low conductance of the Hastings flow meters and the necessity of heating the flow line it was not possible to measure the iodine flow rates in the same manner as for fluorine and argon. Instead, a needle valve was used to meter the iodine vapor and the flow rate determined for various settings of the needle valve by closing the cell to the vacuum pump and observing the rise in pressure with time.

B. Optical system and photon counting apparatus

The wave length of the chemiluminescence was measured with a Jarrell-Ash Ebert scanning monochromator having a focal length of 500 mm and an effective aperture ratio of f/8.6. The instrument was equipped with curved entrance and exit slits. Spectra were obtained at a slit width of 0.35 mm and a full slit height of 20 mm. The grating was ruled at 590 lines/mm resulting in a dispersion of 32 Å/mm and was blazed for maximum intensity at 750 nm in first order. The

monochromator was calibrated between 430 and 720 nm by scanning twenty-two Ne and four Hg atomic lines. Wavelengths were measured to within 0.2 nm throughout the entire wavelength region. The spectral slit function was found (by scanning a number of atomic lines) to be essentially triangular with a full width at half maximum intensity (FWHM) of 1.12 nm.

The slit of the monochromator was positioned ten cm from the 3.8 cm diameter CaF_2 window of the reaction cell. Light from the exit slit of the monochromator was reflected onto the photocathode of an EMI 9558QA photomultiplier tube having an S-20 type spectral response and a quartz window. The field of view of the optical system is indicated in Figure 1. The photomultiplier housing was cooled to dry ice temperatures to reduce the thermionic emission from the large photosensitive area of the photocathode. Photon counting was achieved by use of a Solid State Radiations Model 1120 Amplifier-Discriminator and Model 1105 Data Converter Console. The analog voltage proportional to counts/sec was converted to digital form by a digital voltmeter interfaced to a paper tape punch. Spectra were recorded by a Texas Instruments strip chart recorder and simultaneously as a series of data points punched on paper tape.

The wavelength response of the combined optical and electronic detection system was determined by comparing the spectrum obtained upon scanning the light emitted from a General Electric 30A/T24/17 tungsten ribbon lamp with the

theoretical spectrum. The power supply for the lamp was stabilized by a photo-feed-back system in which light from the ribbon fell onto a photodiode after passing through a blue Corning No. 5030 filter. The temperature of the tungsten ribbon was measured by a Leeds and Northrup optical pyrometer, calibrated by the D.C. Standards section of the Lawrence Berkeley Laboratory. The theoretical spectrum was calculated using the emissivities of tungsten given by DeVos[9]. The intensity correction factor as a function of wavelength which was applied to all spectra is shown in Fig. 2.

To record a spectrum the monochromator was started scanning from 720 nm at 4 nm/min in the direction of decreasing wavelength. Output from the photon counter with an applied time constant of 11.2 seconds was punched every five seconds or 1/3 nm. Thus 870 data points were recorded in the 72.5 minutes required to scan from 720 nm to 430 nm. The punched tapes were converted to punched cards for easy analysis of the data by a CDC 7600/6600 computer[8]. Wavelength and intensity correction factors were applied to all spectra before computer analysis and plotting. Spectra were found to be highly reproducible in spite of the long scanning times.

RESULTS

A. Observation of emission from two excited electronic states of IF

The reaction of molecular iodine with molecular fluorine resulted in a visible yellow-green emission. The conditions

under which seventeen spectra of this emission were recorded are provided in Table I. Spectra were recorded over the wavelength region 430-720 nm for various flow rates of I_2, F_2 and inert gas, Ar. Also included in Table I are the maximum intensities observed for each of the spectra in counts/sec registered by the detector.

Spectra 5 (top) and 9 (bottom) are compared in Figure 3. All of the bands in Spectrum 5 belong to progressions of the $IF(B^3\Pi_{o+} \rightarrow X^1\Sigma^+)$ system described by other investigators.[1,2,3,8] Levels up to at least v' = 8 of the $B^3\Pi_{o+}$ state are populated. In Spectrum 9, which was recorded under different chemical conditions than Spectrum 5, most of the intense bands belong to another band system originating in a bound electronic state of lower energy than the $B^3\Pi_{o+}$ state and terminating in the ground state of IF. Table II is the self-consistent Deslandres table for this new band system. Wavelengths of bands originating in vibrational levels up to v' = 10 were measured, and bands originating in levels up to v' = 16 are indicated, these being appreciably overlapped by bands of the B → X system. We have assigned this banded emission to the $IF(A^3\Pi_1 \rightarrow X^1\Sigma^+)$ transition smilar to that observed for Br_2, I_2, IBr and ICl[4-7]. A least squares fit of the term values to an equation of the form

$$G(v) = \omega_e(v+1/2) - \omega_e x_e(v+1/2)^2$$

gives the results $\omega_e = 380.5\ cm^{-1}$ and $\omega_e x_e = 3.8\ cm^{-1}$ for the $A^3\Pi_1$ state of IF.

It should be noted that the vibrational numbering of the v' levels is not totally unambiguous. For example, it is possible that the level labelled v'=0 is actually v'=1 or some higher level. A vibrational labelling error of this type is much more likely to occur in absorbtion spectroscopy than in emission spectroscopy, however.

B. Effect of varying the flow rates of I_2, F_2 and Ar on the emission spectra

For the nearly stoichiometric flow rates of 24 and 23 std cc/min of fluorine and iodine, respectively, a total pressure of 5.8 mtorr resulted with all of the intense bands observed belonging to the $IF(B^3\Pi_{o+} \rightarrow X^1\Sigma^+)$ transition. Holding the fluorine flow rate at this constant value and lowering the iodine flow rate resulted in a decrease in the emission from the $B^3\Pi_{o+}$ state while emission from the $A^3\Pi_1$ state remained constant. This is demonstrated by the series of spectra 12, 14, 15, 16 and 7 which have been decomposed into components of emission from the A and B states by comparison of the A(5,0) and B(0,3) band intensities (Figure 4).

The effect of varying the flow rate of fluorine was not thoroughly investigated. Spectrum 13 was the only spectrum recorded in which the fluorine flow rate was varied from 24 std. cc/min. The increased flow rate of fluorine in Spectrum 13 compared to that of Spectrum 12 resulted in an increase in total intensity from 939 to 1277 counts/sec with the intensity of emission from each of the two excited electronic states increasing by the same proportion.

The effect of increased Ar pressure on the emission spectra is demonstrated by two series of spectra. In the first series, Spectra 1-5, the iodine flow rate was held at the high value of 16 std cc/min and the flow rate of Ar was

successively increased. In Figure 5a it is seen that the effect of added Ar was an increase in intensity of the $B \rightarrow X$ transition, leveling off at the highest pressures studied. The $A \rightarrow X$ emission, which was a small percentage of the total intensity observed, decreased with increased Ar pressure. Thus at the highest pressure studied (Spectrum 5) the $B \rightarrow X$ spectrum was obtained free of any contamination by $A \rightarrow X$ emission. In a second series of spectra, Spectra 8-11 and 17, the iodine flow rate was held at the low value of 1 std cc/min and the effect of added pressure due to Ar studied. Moderate increases in Ar pressure increased the emission intensity of both the $A \rightarrow X$ and $B \rightarrow X$ systems while higher pressures severely decreased the emission from the $A^3\Pi_1$ state as shown in Figure 5b. The effect of Ar on emission from the $B^3\Pi_{0^+}$ state at lower iodine flow rates is seen to be quite different from that at high iodine flow rates.

Besides increasing the total pressure in the cell, the flow of Ar reduced the pumping speed of the system and thus increased the residence times of all species. The residence time can be computed from the flow rates and total pressure assuming no change in molarity. It varied from 0.2 to 2.0 sec over the range of conditions studied. In the series of spectra in which Ar flow rates were increased while the iodine flow rate was held at the higher constant value (Spectra 1-5), the intensity of the $B \rightarrow X$ emission varied linearly with the cell residence time as can be seen in Figure 6.

C. Determination of vibrational populations and rotational temperatures of the $B^3\Pi_{o+}$ electronic state

If one assumes that a single rotational temperature describes the distribution of molecules among rotational levels, the intensity (quanta/sec) of a vibration-rotation line in spontaneous emission may be shown to be[10]

$$I_{v''J''}^{v'J'} = \frac{64\pi^4 B_{v'} S_{J''}^{J'}}{3hkT_r} \exp\left[-\frac{B_{v'}J'(J'+1)}{kT_r}\right] \nu^3 \langle v'|Re|v''\rangle^2 N_{v'} \qquad (1)$$

where $B_{v'}$ is the rotational spectroscopic constant for vibrational level v', $N_{v'}$ is the vibrational population of level v', T_r is the rotational temperature, ν is the frequency of the emission line, R_e is the transition moment and $S_{J''}^{J'}$ is the Honl-London factor. For a transition of the type $0^+ \rightarrow 0^+$ the Honl-London factors are given by

$$\begin{aligned} R_{branch} \qquad & S_{J''}^{J'} = J' \\ P_{branch} \qquad & S_{J''}^{J'} = J' + 1 \end{aligned} \qquad (2)$$

Relative vibrational populations can be determined from relative spectral intensities if the transition moment matrix elements are known. A common practice is to apply the Born-Oppenheimer[11] approximation in which the electronic wavefunction is considered to be only weakly dependent on the internuclear distance. The square of the electronic transition moment may then be removed from under the integral and be considered to take on an average value $\bar{R}_e^2$.

$$\langle v'|Re|v''\rangle^2 \approx \bar{R}_e^2 \langle v'|v''\rangle^2 \qquad (3)$$

This approximation was not found to be sufficiently accurate for the IF($B^3\Pi_{o+} \rightarrow X^1\Sigma^+$) transition. A better approximation is that due to Fraser[12] and Turner and Nicholls[13]. In this method the transition moment is considered to be a function of the quantum mechanical average value of the internuclear distance called the $\bar{r}$-centroid. Thus,

$$\langle v'|Re(r)|v''\rangle \tilde{\propto} Re^2(\bar{r}_{v'v''}) \langle v'|v''\rangle^2 \qquad (4)$$

where the $\bar{r}$-centroid is evaluated for each band in the system and is given by:

$$\bar{r}_{v'v''} = \frac{\langle v'|r|v''\rangle}{\langle v'|v''\rangle} \qquad (5)$$

We have calculated the Franck-Condon factors $\langle v'|v''\rangle$ and $\bar{r}$-centroids by the RKR method using the computer programs of Zare[14]. The results are tabulated in Table III. For a given progression of bands having a common upper vibrational level the band intensities differ only by ν^3, the Franck-Condon factor, and the value of the transition moment. The square of the transition moment was evaluated as a function of the $\bar{r}$-centroid by plotting the maximum intensity of each band in a given progression of bands divided by ν^3 and the appropriate Franck-Condon factor against the $\bar{r}$-centroid for that particular band. The curve thus obtained for each progression was normalized so that the area under all such curves was the same. The normalization factors are, of course, the relative vibrational populations. Spectrum 5 was used for this determination of the transition moment as a function of the $\bar{r}$-centroid since it

is free of contamination by the A → X system. Only progressions having v' = 0,1 and 2 could be used for this purpose since there was an insufficient number of observed bands in progressions having v'>2. These progressions gave relative values of $R_e^2(\bar{r})$ for values of $\bar{r}$ between 1.975 and 2.234 Å. Relative vibrational populations of levels v' = 0,1 and 2 were found to be 1.00, 0.62 and 0.46 respectively. The square of the transition moment was found to vary linearly with the $\bar{r}$-centroid as can be seen in Figure 7. To determine the vibrational populations of levels v' = 3 to v' = 8 it was necessary to rely on a short linear extrapolation of the $R_e^2(r)$ curve to smaller values of the $\bar{r}$-centroid.

For each vibrational band, theoretical band shapes were calculated for various assumed rotational temperatures by taking the convolution of the experimentally derived RC-broadened spectral slit function with the relative intensities of all rotational lines within a 20 nm envelope containing the band head[8]. The theoretical shapes of the B(0,4) band for three rotational temperatures are given in Figure 8. These have been normalized by the maximum band intensity. The relative rotational line intensities are given by equation 1 without the factor $\langle v'|R_e|v''\rangle^2 N_{v'}$. By comparing the theoretical band shapes with the experimental results it was possible to determine rotational temperatures to within 100 K.

Once a rotational temperature had been decided upon, the vibrational populations for levels v' = 0 to v' = 8 of the $B^3\Pi_{o+}$ state were determined by use of a least squares computer program which fit the theoretical band shapes [after multiplying the band intensities by the appropriate Franck-Condon factor and value of R_e^2 $(\bar{r})$] to the ∿850 spectral data points, the fitting parameters being the relative vibrational populations. In this method B_i is the total observed intensity after correction for the spectral sensitivity of the optical system, and N_j is the population of the vibrational level v' = j. We may then write

$$B_i = \sum_j A_{ij} N_j \qquad (6)$$

where the term A_{ij} is the contribution to the intensity at λ_i by all bands for which v' = j. That is,

$$A_{ij} = \sum_{v''} T(v',v'')\, R_e^{\,2}\, (\bar{r}_{jv''})\, \langle j|v''\rangle^2$$

where T(v',v") is the intensity of the normalized band (v',v") at wavelength λ_i. There are only one or two terms in the sum since there is very little overlap between bands originating in the same vibrational level. In general, the number of measurements of the intensity, m (∿850), is much greater than the number of fitting parameters, the vibrational populations (∿9). In order to solve the over-determined set of simultaneous equations, the method of least squares is used. A set of N_j's are found which satisfy the criteria

$$\frac{\partial}{\partial N_j} \left(\sum_{i=1}^{m} \left(B_i - \sum_{j=0}^{n-1} A_{ij} N_j \right)^2 w_i \right) = 0 \quad j = 0,1,\ldots n \qquad (8)$$

where w_i is a weighting factor, chosen to be the inverse of the square of the standard deviation of the measurement. Since

noise in the signal varies as the square root of the signal, the weighting factor was taken to be the reciprocal of the intensity itself. A least squares variable metric minimization program was used as a subroutine in a computer program written to determine the vibrational populations in the manner described[8].

For spectra which were overlapped by bands from the A → X transition various amounts of Spectrum 9 were subtracted from the spectrum to be fit prior to determining the vibrational populations by the least squares computer program. The fit which gave the least variance yielded the relative emission from the two excited electronic states as well as the vibrational populations of the $B^3\Pi_{o+}$ state.

Vibrational populations for Spectra 1-5 were determined in the manner just described. In this series of spectra, increasing amounts of pressure due to Ar were added with flow rates of I_2 and F_2 held constant, but the cell residence time also varied, as was previously pointed out. The vibrational populations, vibrational temperatures, rotational temperatures and fractional amounts of A → X emission for this series of five spectra are presented in Table IV. For the highest pressure spectrum (Spectrum 5) the vibrational populations can be described well by a vibrational temperature of ~1250 K. At lower pressures the populations become non-Boltzmann, and the vibrational level v' = 1 becomes inverted over v' = 0. The lowest and highest pressure spectra of this series are

shown in Figures 9a and 9b and the spectra computed from the vibrational populations and theoretical band shapes compared with the spectral data. There is good agreement between the computed spectra and experimentally derived spectra for Spectra 3,4, and 5. The fits to Spectra 1 and 2 are not nearly as good. This is possibly due to changes in vibrational populations of the $A^3\Pi_1$ state with pressure. That is, the low pressure Spectra 1 and 2 are contaminated by emission from the $A^3\Pi_1$ state with different vibrational populations than in Spectrum 9. As a result, correction by the use of Spectrum 9 cannot be exact. In the least squares fit some bands will be overly compensated for, while for others there is an undercompensation. This source of error does not result in a very serious effect on the calculated vibrational population of the B state, however, since the calculated vibrational populations were found to be affected only to a small extent by the amount of spectrum 9 subtracted out.

DISCUSSION

A. Assignment of emission to electronic states and the ground state dissociation energy of IF.

All of the visible/near IR banded emission and absorbtion spectra of the halogen and interhalogen diatomic molecules have been successfully assigned thus far as transitions between the ground $X^1\Sigma^+$ state

and a $B^3\Pi_{o+}$ or $A^3\Pi_1$ excited electronic state.[21] Transitions between the ground electronic state and the $^3\Pi_{o-}$ and $^3\Pi_2$ states have not been observed apparently due to operation of the selection rules $+ \not\leftrightarrow -$ and $\Delta\Omega = 0, \pm 1$. The spin selection rule, $\Delta S = 0$, does not hold strictly for heavy halogen molecules in which there is strong spin-orbit coupling. The $A^3\Pi_1$ state correlates with ground state atoms, and the $B^3\Pi_{o+}$ state correlates with one ground state $^2P_{3/2}$ atom and one spin-orbit excited $^2P_{1/2}$ atom. For interhalogen molecules XY there are two possible diabatic $^3\Pi_{o+}$ states that correlate with $X(^2P_{1/2})$ and $Y(^2P_{1/2})$ products, respectively. There is also a repulsive state of 0^+ symmetry that correlates with ground state atoms. Interaction of the $B^3\Pi_{o+}$ state with this $Y(0^+)$ state can lead to the formation of a new $B'(0^+)$ state as in the cases of IBr[16], ICl[17], and BrF[18].

The accurate determination of the dissociation energy of the ground electronic state for the halogens and interhalogens has in most cases been accomplished by means of a Birge-Sponer extrapolation of one of the excited electronic states. One requires in addition, knowledge of the frequency of the (0,0) band and the dissociation products of the upper state. If the upper electronic state is that of $^3\Pi_1$ there is no problem since both this state and the ground state dissociate to ground state atoms. In the case of a $^3\Pi_{o+}$ upper state, however, there are two possibilities for the dissociation products. Durie[2] obtained the value 4680 ± 100 cm^{-1} for the dissociation energy of the $B^3\Pi_{o+}$ state of IF by means of a Birge-Sponer extrapolation, and concluded that the dissociation energy for the

ground state of IF must be either 16035 ± 100 cm^{-1} or 23229 ± 100 cm^{-1} depending upon the dissociation products of the upper state as illustrated in figure 10. A new band system belonging to an excited electronic state whose minimum lies 3348 cm^{-1} below the minimum in the $B^3\Pi_{o+}$ potential energy curve has been described here. This new band system may originate in the $A^3\Pi_1$ state, or in the case that the $B^3\Pi_{o+}$ state correlates with I* + F it may be the lower lying $^3\Pi_{o+}$ state correlating with I + F*. At least eight vibrational levels of this new state lie above both the value 16035 cm^{-1} and the value 16439 cm^{-1} which are the dissociation limits for the $A^3\Pi_1$ state and the lower lying $^3\Pi_{o+}$ state in the case that the $B^3\Pi_{o+}$ state correlates with I* + F. Thus it would follow that the $B^3\Pi_{o+}$ state must correlate with I + F*, and the new band system originates in the $A^3\Pi_1$ state.

The reliability of the graphical Birge-Sponer extrapolation for the $B^3\Pi_{o+}$ state of IF is questionable, however, since a similar extrapolation by Durie[1] for the $B^3\Pi_{o+}$ state of BrF was found by Brodersen and Sicre[18] to be low due to the crossing of the $B^3\Pi_{o+}$ state by two repulsive curves of 0^+ symmetry. In the absorbtion spectrum Brodersen and Sicre[18] found the convergence limits of both the $A^3\Pi_1 \leftarrow X^1\Sigma^+$ system and the $B^3\Pi_{o+} \leftarrow X^1\Sigma^+$ system observed in emission by Durie[1]. The difference in the convergence limits differed by a value of 3748 ± 60 cm^{-1} which is very close to the excitation energy of a $Br(^2P_{1/2})$ atom (3865 cm^{-1}). They interpreted

all vibrational levels from v' = 6 to v' = 15 of the $B^3\Pi_{o+}$ state to be strongly perturbed by another electronic state in the vicinity of v' = 12. This perturbation led to an anomalously low estimate by Durie[1] for the dissociation energy of the $B^3\Pi_{o+}$ state of BrF since he observed levels up to only v' = 9 in emission.

In the case of IF, Durie[2] found that predissociation begins at J = 45 in the v' = 11 level of the $B^3\Pi_{o+}$ state, thus establishing that the ground state dissociation energy of IF is definitely less than 23341 cm^{-1}. No emission was observed from v' = 12 or higher levels and there were only slight perturbations in the rotational constants for the v' = 9 and 10 levels. No predissociation occurred in the v' = 9 and 10 levels even though rotational levels far above the predissociation limit were observed. The onset of predissociation at 23341 cm^{-1} is highly coincident with the higher value for the ground state dissociation energy of 23229 cm^{-1} once the rotational energy barrier of 94 cm^{-1} for J = 45 is taken into account. Durie[2] argued that this suggested that the $B^3\Pi_{o+}$ state is perturbed by a state crossing nearly horizontally quite unlike the cases of BrF[18], IBr[16] and ICl[17]. Child and Bernstein[19] have pointed out several systematic trends in the potential energy curves for the halogens and interhalogens. For example, the dissociation energies of the $B^3\Pi_{o+}$ states of I_2, IBr and ICl are 4507 cm^{-1}, 2243 cm^{-1} and 799 cm^{-1} respectively. These states all correlate

with a ground state I atom, the remaining atom being spin-orbit excited. This suggests that the $^3\Pi_{o+}$ state of IF correlating with a ground state I atom and a spin-orbit excited F* atom is at best very weakly bound. For this reason Child and Bernstein[19] concluded that the $B^3\Pi_{o+}$ state correlates with a ground state F atom and an excited I* atom, the low convergence limit being due to a crossing with a repulsive state of 0^+ symmetry resulting in a potential maximum as illustrated by Figure 11a (drawn for the special case, $D_o'' = 23229\ cm^{-1}$). This would lead to a much stronger perturbation in the rotational structure than that observed by Durie[2], however, since such a crossing would be expected to perturb many vibrational levels. Also, for this case the ground state dissociation energy is uncertain and is only known to lie between the values 16035 cm^{-1} and 23229 cm^{-1}. A scheme is proposed here which is consistent with the type of predissociation observed by Durie[2]. This scheme is illustrated by Figure 11b in which a weakly bound $^3\Pi_{o+}$ state correlating with a ground state I atom and a spin-orbit excited F* atom has been added to Figure 10a resulting in an additional avoided curve crossing. Thus, the spectroscopically observed $B^3\Pi_{o+}$ state correlates diabatically with I* + F as suggested by Child and Bernstein[19], and adiabatically with I + F* according to this scheme. The forced correlation would result in strong curvature of the Birge-Sponer extrapolation as was observed, and predissociation would be expected to begin at an energy slightly larger than the

dissociation energy of 23229 cm^{-1}. Coxon[22] has placed a lower limit of 23103 cm^{-1} on D_o'', based on a third degree polynomial fit to the data presented here (Table II) for the vibrational spacings of the $A^3\Pi_1$ state. Combining this result with the upper limit of 23341 cm^{-1}, the predissociation limit, we obtain $D_o'' = 23222 \pm 120$ cm^{-1} in excellent agreement with the value 23229 ± 100 cm^{-1} (Figure 10b).

The value of 23229 cm^{-1} for the dissociation energy of the ground state of IF leads to the values of 7638 cm^{-1} for the dissociation energy of the $A^3\Pi_1$ state and 11874 cm^{-1} for the diabatic dissociation energy of the $B^3\Pi_{o+}$ state. The value of 7638 cm^{-1} for the dissociation energy of the $A^3\Pi_1$ state follows the trend set by I_2, IBr, and ICl of 658 cm^{-1}, 2375 cm^{-1}, and 3684 cm^{-1}, respectively. The same series of molecules give 12440 cm^{-1}, 14660 cm^{-1}, and 17340 cm^{-1} for the dissociation energies of the ground state. The value of 23229 cm^{-1} is consistent with this trend in which the increasing bond energies are due to the increasing differences in electronegativities of the two atoms.

D. Mechanism of population of the $A^3\Pi_1$ and $B^3\Pi_{o+}$ states of IF

If one considers the energetics of the possible reactions between molecules consisting of iodine and fluorine atoms, one finds that there are only two possible mechanisms for the population of excited electronic states of IF in the reaction of I_2 with F_2 for a flow system such as the one described here. This is unlike the situation in an iodine-fluorine flame in which the exothermicity of the overall reaction

$$1/2\ I_2 + 5/2\ F_2 \rightarrow IF_5 \quad \Delta H = -205 \text{ kcal/mole} \qquad (9)$$

is available to reaction processes by way of the high flame temperature. The first of these possible reactions is the following

$$I_2 + F_2 \rightarrow IF^* + IF \qquad (10)$$

where IF* is an IF molecule in either the $A^3\Pi_1$ or $B^3\Pi_{o+}$ electronic state. Considering the bond energies of I_2, F_2 and the value of the bond energy for IF adopted here, emission from IF* can occur at wavelengths as short as 472±5 nm. This coincides well with the short wavelength cutoff in emission from both the $A^3\Pi_1$ and $B^3\Pi_{o+}$. Of course, this reaction would proceed through a four-center transition complex and for this reason should be considered with some skepticism.

The second possible mechanism for the population of excited electronic states is that of three-body recombination of I and F atoms. The reactions

$$I_2 + F_2 \rightarrow IF_2 + I \qquad (11)$$

$$IF_2 + F_2 \rightarrow IF_3 + F \qquad (12)$$

$$IF_n + F_2 \rightarrow IF_{n+1} + F \text{ in general for } n \leq 4 \qquad (13)$$

are probable sources of I and F atoms. Of the two reactions

$$F + I_2 \rightarrow IF + I \qquad (14)$$

$$I + F_2 \rightarrow IF + F \qquad (15)$$

the first is expected to be faster than the second since $F + Cl_2$ is much faster than $Cl + F_2$[15]. These two reactions may propagate a long chain in the explosive reaction between I_2 and F_2 if the second reaction is sufficiently fast. Neither of these reactions is exothermic enough to populate excited electronic states. Since at 300 K there are substantial amounts ($\sim$ 13%) of $F(^2P_{1/2})$ atoms in thermal equilibrium with $F(^2P_{3/2})$ atoms both the $A^3\Pi_1$ and $B^3\Pi_{o+}$ states may be populated up to their dissociation limits by atom recombination provided that the value of 23229 $\pm$ 100 cm^{-1} assumed here for the dissociation energy of the ground state is correct. If the dissociation energy is less than this value then atoms must pass over or tunnel through a potential barrier to populate the $B^3\Pi_{o+}$ state. The rate of population of the $B^3\Pi_{o+}$ state compared to that of the $A^3\Pi_1$ state would be negligible for an energy barrier of more than a few hundred wavenumbers. Thus for the atom recombination mechanism the fact that the reaction between I_2 and F_2 populates the $B^3\Pi_{o+}$ state of IF favors the highest possible value for the dissociation energy.

Clyne, Coxon and Woon-Fat[5] have studied the recombination of $Br(^2P_{3/2})$ atoms in the presence of singlet $O_2(^1\Delta_g, ^1\Sigma^+_g)$, and

Clyne, Coxon and Townsend[3] have studied the recombination of $Br(^2P_{3/2})$ atoms with $F(^2P_{3/2},^2P_{1/2})$ atoms and the recombination of $I(^2P_{3/2})$ atoms with $F(^2P_{3/2}, ^2P_{1/2})$ atoms, both in the presence of singlet $O_2(^1\Delta_g, ^1\Sigma_g^+)$. Singlet oxygen greatly enhanced the emission from the $B^3\Pi_{o+}$ state in the case of Br_2 and was explicitly required for emission from the $B^3\Pi_{o+}$ state in the case of BrF. For both Br_2 and BrF there is an energy barrier to atom recombination which is overcome by energy transfer from singlet oxygen. Unfortunately, no determination was made as to whether singlet $O_2(^1\Delta_g, ^1\Sigma_g^+)$ was explicitly required for emission from the $B^3\Pi_{o+}$ state in the recombination of I and F atoms.

The recombination of I and F atoms in the presence of a third body M

$$I + F + M \xrightarrow{a} IF^* + M \qquad (16)$$

may be followed by collisional quenching of IF*

$$IF^* + M \xrightarrow{b} IF + M \qquad (17)$$

or by radiative transfer to the ground state.

$$IF^* \xrightarrow{c} IF + h\nu \qquad (18)$$

These three reactions lead to the following for the steady state concentration of IF*:

$$(IF^*) = \frac{a(I)(F)(M)}{b(M) + c} \qquad (19)$$

If one assumes that I and F atoms are terminated primarily by the atom recombination steps I+F+M, I+I+M, and F+F+M one finds that:

$$(IF^*) \propto \frac{(I_2)(F_2)}{b(M) + c} \qquad (20)$$

This expression is the same as that which one arrives at for the first mechanism discussed, which involves a four-center reaction between I_2 and F_2. The difference in the dependence of the $A^3\Pi_1$ and $B^3\Pi_{o+}$ emission on the concentration of I_2 (figure 5) can be explained on the basis of the radiative lifetimes of the two states, according to equation 20, if I_2 is primarily responsible for electronic quenching so that $I_2 \equiv M$. In the case that emission from the $A^3\Pi_1$ state is in the high pressure limit of equation 20 then the dependence on (I_2) is removed, as was observed. The $B^3\Pi_{o+}$ state must be in the low pressure limit to fit the experimental results, thus predicting that the $A^3\Pi_1$ state, has a much longer radiative life-time than the $B^3\Pi_{o+}$ state for similar quenching constants. As will be discussed below, the radiative lifetime of the $B^3\Pi_{o+}$ state is short enough to be competitive with the vibrational relaxation time at the pressures studied. Addition of an inert gas such as Ar would be expected to decrease emission from the $A^3\Pi_1$ state at sufficiently high pressures, as was observed (Figures 6 and 7). Small flow rates of Ar would be expected to increase emission from the $A^3\Pi_1$ state by increasing the cell residence time and thus the F_2 concentration. Increasing flow rates of Ar would be expected to increase the emission from the $B^3\Pi_{o+}$ state by increasing both the concentrations of F_2 and I_2. Thus the effect of flow rates of F_2, I_2 and Ar on the relative emission

from these two excited electronic states can be explained in a qualitative way by either of the two mechanisms discussed. For the atom recombination mechanism, however, it is more likely that F atoms are terminated by reaction 14 and I atoms terminated by I + I + M, in which case the changes in spectral intensities with changes in gas flow rates are not readily explained. This fact, combined with the coincidence of the emission cutoff with that expected for the four-center complex mechnism, supports reaction 10 as the mechnism of population of excited states of IF in the reaction between I_2 and F_2.

E. Effect of Pressure on Vibrational Populations of the $B^3\Pi_{o+}$ State

The vibrational populations for Spectra 1-5 are given in Table 5 and the vibrational populations for the two extremes in pressure are compared graphically in Figure 12. For this series of spectra the flow rates of I_2 and F_2 into the cell were held constant and the total pressure increased from the value of 4.8 mtorr to as high as 310 mtorr by an increased flow of Ar. Increasing the flow rate of Ar increased the cell residence time by decreasing the pumping speed of the system and thus increased concentrations of I_2, F_2, and reaction products in the cell, as discussed previously. For this reason changes in vibrational populations cannot be attributed solely to increased pressures of Ar, and in fact are probably due to the increased pressures of halogens and interhalogens as these molecules are excellent energy transfer agents. For this reason the effect of increased pressure on the vibrational populations will only be discussed in a qualitative manner.

Increasing the pressure to 310 mtorr with Ar increased the cell residence time from 0.2 to 1.6 sec (Figure 8) so that the pressure of halogens increased from about 5 to 40 mtorr. Moderate pressures (up to 32 mtorr) of Ar (Spectra 2 and 3) had little effect on the cell residence time and little effect on the vibrational populations (Table 5). The substantial changes in vibrational populations brought on by larger flow rates of Ar (Spectra 4 and 5) appear to be due to the increased deactivation by halogens and interhalogens as a result of the increased cell residence times.

Measurement of vibrational relaxation times of homonuclear halogens by Millikan and White[20] resulted in a typical value of 10^{-7} for $p\tau_V$ where p is the pressure in atmospheres and τ_V is the vibrational relaxation time. The vibrational populations change substantially over the halogen pressure range of 5 to 40 mtorr so that over this pressure range the radiative lifetime must be competitive with the vibrational relaxation time. This yields a radiative lifetime of about one millisecond for the $B^3\Pi_{o+}$ state of IF. The cell residence time is long compared to this value for the radiative lifetime so that essentially all molecules formed in excited states emit before passing out of the cell.

A radiative lifetime of about one millisecond for the $B^3\Pi_{o+}$ state of IF is intermediate between that of I_2 (7×10^{-7})[28] and that of F_2 which has not been measured, but is expected to be very long due to the forbiddenness of the transition which

only becomes allowed for heavy molecules for which there is strong spin-orbit coupling. Coxon[21] has estimated the radiative lifetime of F_2 to be 0.3 sec.

The lowest pressure spectrum, Spectrum 1, is non-Boltzmann and exhibits a slight population inversion for v' = 1. One goal of this study was to obtain the "initial distribution" of molecules among vibrational energy levels. In the low pressure limit a newly formed molecule will radiate before colliding with another molecule so that the vibrational populations represent the rates of reaction into each of the vibrational levels. In atom recombination the higher vibrational levels are populated at a more rapid rate than lower vibrational levels, and one would expect the initial distribution to be highly inverted. In these experiments the trend with reduced pressure is clearly in this direction, but the vibrational distribution is far from that expected for the initial distribution. This is despite a reduction in total pressure by an order of magnitude over that used by Gabelnick[8] and an increased cell volume from 1 to 350 liters to reduce deactivation at the walls. Thus, the behavior of the vibrational populations with changes in pressure is in better accord with the four-center reaction mechanism than with the atom association mechanism. Further kinetic studies are necessary in order to elucidate the mechanism of population of excited electronic states in this interesting reaction.

Acknowledgments

This work was done under the auspices of the U. S. Atomic Energy Commission.

REFERENCES

1. R. A. Durie, Proc. R. Soc. A 207, 388 (1951).
2. R. A. Durie, Can. J. Phys. 44, 337 (1966).
3. M. A. A. Clyne, J. A. Coxon and L. W. Townsend, J. Chem. Soc. Faraday Trans. II 68, 2134 (1972).
4. M. A. A. Clyne and J. A. Coxon, J. Mol. Spec. 23, 258 (1967).
5. M. A. A. Clyne, J. A. Coxon and A. R. Woon-Fat, Trans. Far. Soc. 67, 3155 (1971).
6. M. A. A. Clyne and J. A. Coxon, Proc. R. Soc. A 298, 424 (1967).
7. R. J. Browne and E. A. Ogryzlo, J. Chem. Phys. 52, 5774 (1970).
8. S. D. Gabelnick, Ph.D. Thesis, University of California, Berkeley, Lawrence Berkeley Laboratory Report UCRL-18623 (1969).
9. J. C. DeVos, Physica 20, 690 (1954).
10. G. Herzberg, Molecular Spectra and Molecular Structure I. Spectra of Diatomic Molecules, 2nd ed. (Van Nostrand, Princeton, 1950).
11. M. Born and R. Oppenheimer, Ann. Physik 84, 457 (1927).
12. P. A. Fraser, Can. J. Phys. 32, 515 (1954).
13. R. G. Turner and R. W. Nicholls, Can. J. Phys. 32, 475 (1954).
14. R. N. Zare, Lawrence Berkeley Laboratory Report UCRL-10925 (1963).
15. R. T. Watson, Private Communication.
16. W. G. Brown, Phys. Rev. 42, 355 (1932).
17. W. G. Brown and G. E. Gibson, Phys. Rev. 40, 529 (1932).
18. P. H. Brodersen and J. E. Sicre, Z. Phys. 141, 515 (1955).
19. M. S. Child and R. B. Bernstein, J. Chem. Phys. 59, 5916 (1973).
20. R. C. Millikan and D. R. White, J. Chem. Phys. 39, 3209 (1963).
21. J. A. Coxon, Chem. Soc. Spec. Rep., Molec. Spec. 1, Chapter 4 (1972).
22. J. A. Coxon, private communication.

Table I. Values of Flow Rates, Total Pressure, and Maximum Intensity for the Seventeen Spectra

Spectrum No.	Flow Rates (Std. cc/min)			Total Pressure (mtorr)	Maximum Intensity (counts/sec)
	I_2	F_2	Ar		
1	16.0	24	0	4.75	887
2	"	"	56	12.8	694
3	"	"	68	32.0	1230
4	"	"	89	115	2338
5	"	"	>100	310	2754
6	"	"	0	4.2	681
7	1.0	"	0	3.8	220
8	"	"	0	3.4	205
9	"	"	29	10.0	210
10	"	"	>100	180	81
11	"	"	70	18.1	240
12	23.0	"	0	5.8	939
13	"	42	"	6.7	1277
14	16.0	24	"	4.8	700
15	6.7	"	"	4.2	461
16	2.9	"	"	4.0	311
17	1.0	"	80	70.	110

Table II

Deslandres Table for IF($^3\Pi_1 \rightarrow {}^1\Sigma^+$)

v' \ v''	0		1		2
0	15591 (371)	(607)	14984 (370)	(598)	14386
1	15962 (365)	(608)	15354 (364)		
2	16327 (362)	(609)	15718		
3	16689 (347)				
4	17036 (343)				
5	17379 (336)				
6	17715 (332)				
7	18047 (318)				
8	18365 (306)				
9	18671 (308)				
10	18979				

Table III

Franck-Condon Factors and Values of the $\bar{r}$-Centroid for the B → X Band System of IF. Upper value is the Franck-Condon Factor. Lower value is the $\bar{r}$-centroid in Angstroms.

v'' \ v'	0	1	2	3	4	5	6	7	8
0	5.000-3* 2.007	2.245-2 1.991	5.302-2 1.975	8.919-2 1.960	1.195-1 1.946	1.342-1 1.932	1.316-1 1.918	1.160-1 1.905	9.456-2 1.892
1	3.039-2 2.031	9.015-2 2.014	1.307-1 1.998	1.202-1 1.983	7.176-2 1.986	2.268-2 1.953	5.947-4 1.935	7.707-3 1.928	3.008-2 1.915
2	8.784-2 2.055	1.493-1 2.038	9.737-2 2.021	1.889-2 2.003	2.891-3 1.998	3.831-2 1.978	6.704-2 1.963	6.092-2 1.949	3.343-2 1.936
3	1.602-1 2.080	1.183-1 2.061	7.914-3 2.039	2.464-2 2.032	7.322-2 2.014	5.547-2 1.998	1.153-2 1.982	1.660-3 1.980	2.405-2 1.960
4	2.065-1 2.105	3.059-2 2.084	2.965-2 2.073	8.448-2 2.053	3.050-2 2.035	1.035-3 2.038	3.567-2 2.009	5.410-2 1.994	3.098-2 1.979
5	1.998-1 2.131	3.013-3 2.125	9.732-2 2.095	2.850-2 2.074	1.032-2 2.068	5.935-2 2.046	3.822-2 2.029	1.524-3 2.003	1.303-2 2.006
6	1.507-1 2.158	6.710-2 2.142	6.683-2 2.119	7.922-3 2.112	7.015-2 2.086	2.319-2 2.066	4.745-3 2.064	4.274-2 2.041	3.920-2 2.024
7	9.057-2 2.186	1.423-1 2.168	3.554-3 2.134	7.558-2 2.130	2.783-2 2.107	1.307-2 2.101	5.573-2 2.078	1.934-2 2.059	1.904-3 2.063
8	4.400-2 2.215	1.572-1 2.195	2.915-2 2.180	6.923-2 2.154	7.234-3 2.147	6.452-2 2.119	1.037-2 2.095	1.596-2 2.092	4.550-2 2.072
9	1.742-2 2.246	1.167-1 2.224	1.103-1 2.205	6.309-3 2.171	7.149-2 2.165	1.705-2 2.139	2.450-2 2.133	4.833-2 2.111	3.729-3 2.082
10	5.667-3 2.278	6.391-2 2.254	1.478-1 2.234	2.388-2 2.218	6.012-2 2.189	1.487-2 2.180	5.769-2 2.153	8.129-4 2.101	3.269-2 2.124

*Abbreviated notation for 5.000×10^{-3}

Table IV. Vibrational Populations, Vibrational Temperatures, Rotational Temperatures, and fractional amounts, f, of Spectrum 9 subtracted. Upper value is the relative vibrational population. Lower value is the calculated vibrational temperature temperature relative to v' = 0.

v'=	Spectrum 1	Spectrum 2	Spectrum 3	Spectrum 4	Spectrum 5
0	1.00	1.00	1.00	1.00	1.00
1	1.04±.03 -1481$\bar{7}$	1.01±.02 -584$\bar{0}$	.91±.02 616$\bar{2}$	.71±.01 169$\bar{7}$	.62±.01 121$\bar{6}$
2	.81±.03 548$\bar{8}$	.78±.02 465$\bar{5}$	.73±.02 367$\bar{5}$	.49±.01 162$\bar{1}$	.46±.01 148$\bar{9}$
3	.54±.05 278$\bar{7}$	.53±.04 270$\bar{5}$	.50±.03 247$\bar{8}$	.30±.02 240$\bar{8}$	.27 ±.02 131$\bar{2}$
4	.36±.06 222$\bar{5}$	.33±.05 205$\bar{0}$	.32±.04 199$\bar{5}$	.18±.02 132$\bar{5}$	.16±.03 124$\bar{0}$
5	.21±.08 180$\bar{4}$	.17±.06 158$\bar{9}$	.19±.05 169$\bar{5}$	.11±.03 127$\bar{5}$	.10±.03 122$\bar{3}$
6	.14±.09 170$\bar{2}$	.09±.07 138$\bar{9}$	.12±.06 157$\bar{8}$	.06±.04 118$\bar{9}$	.06±.04 118$\bar{9}$
7	.06±.13 137$\bar{3}$	.03±.10 110$\bar{2}$	.04±.08 120$\bar{0}$	.03±.05 110$\bar{2}$	.04±.06 120$\bar{0}$
8	.01±.26 94$\bar{8}$	.01±.25 94$\bar{8}$	.02±.19 111$\bar{6}$	<.01	.03±.14 124$\bar{5}$
f	.47	.45	.34	.14	0.
T_r	400-500 K	400-500 K	~500 K	~500 K	500-600 K

FIGURE TITLES

Figure 1. Schematic Diagram of the Apparatus

Figure 2. Intensity Correction Factor Applied to Spectra

Figure 3. Comparison of Spectra 5 (Upper) and 9 (Lower). Positions of the B→X emission bands are indicated in Spectrum 5, and positions of the A→X bands are indicated in Spectrum 9. As can be seen, Spectrum 9 is somewhat contaminated by emission from the B state.

Figure 4. Effect of Pressure Due to I_2 on Emission from the A and B States as Measured by the A(5,0) and B(0,3) Band Intensities

Figure 5a. Effect of Increased Pressure Due to Ar on Emission from the A and B States for the Higher I_2 Flow Rate

Figure 5b. Effect of Pressure Due to Ar on Emission from the A and B States for the Lower I_2 Flow Rate. Compare the intensity scales of Figures 4, 5a and 5b.

Figure 6. Plot of the B(0,3) Band Intensity Against the Cell Residence Time. Compare with Figure 5a in which a plot against pressure was strongly curved.

Figure 7. Variation of the Square of the Transition Moment with the r-Centroid. ● evaluated from the progression originating in v' = 0, □ evaluated from the progression originating in v' = 1, and ▲ evaluated from the progression originating in v' = 2.

Figure 8. Theoretical Shapes of the B(0,4) Band Calculated for Three Rotational Temperatures.

Figure 9a. Comparison of Computed Spectrum with the Observed Points for Spectrum 1. Total pressure for this spectrum is 4.75 mtorr.

Figure 9b. Comparison of Computed Spectrum with the Observed Points for Spectrum 5. Total pressure for this spectrum is 310 mtorr.

Figure 10. Combining the Dissociation Energy of the $B^3\Pi_{0+}$ State with the Energy of the (0,0) Band and Subtracting the Two Possible Spin-Orbit Excitation Energies Leads to the Possible Values 23229 cm^{-1} and 16035 cm^{-1} for the Ground State Dissociation Energy of IF.

Figure 11a Potential Energy Curves Drawn for IF in the Case that the $B^3\Pi_{0+}$ State Correlates diabatically with I*+F. The $B^3\Pi_{0^+}$ state is forced to correlate adiabatically with ground state atoms due to an avoided crossing with a repulsive state of 0^+ symmetry. In this case the ground state dissociation energy is only known to lie between the values 16035 cm^{-1} and 23229 cm^{-1}. Predissociation in the emission spectra would be expected to begin well below the convergence limit, however, due to tunneling through the potential barrier as in the case of BrF.[18] This figure is drawn for the special case, D''_o = 23229 cm^{-1}.

Figure 11b Potential Energy Curves for IF. In this case an additional weakly bound $^3\Pi_{0^+}$ state has been drawn which leads to an avoided crossing with the $^3\Pi_{0^+}$ state of Figure 11a. The avoided crossing results in a forced correlation of the strongly bound $^3\Pi_{0+}$ state with the products I + F*. In this case the ground state dissociation energy is known exactly to be 23229 cm^{-1} from Figure 10, there should be a strongly curved Birge-Sponer extrapolation, and predissociation cannot occur below the dissociation limit.

Figure 12. Comparison of Vibrational Populations Calculated from Spectra 1 and 5.

Schematic Diagram of the Apparatus

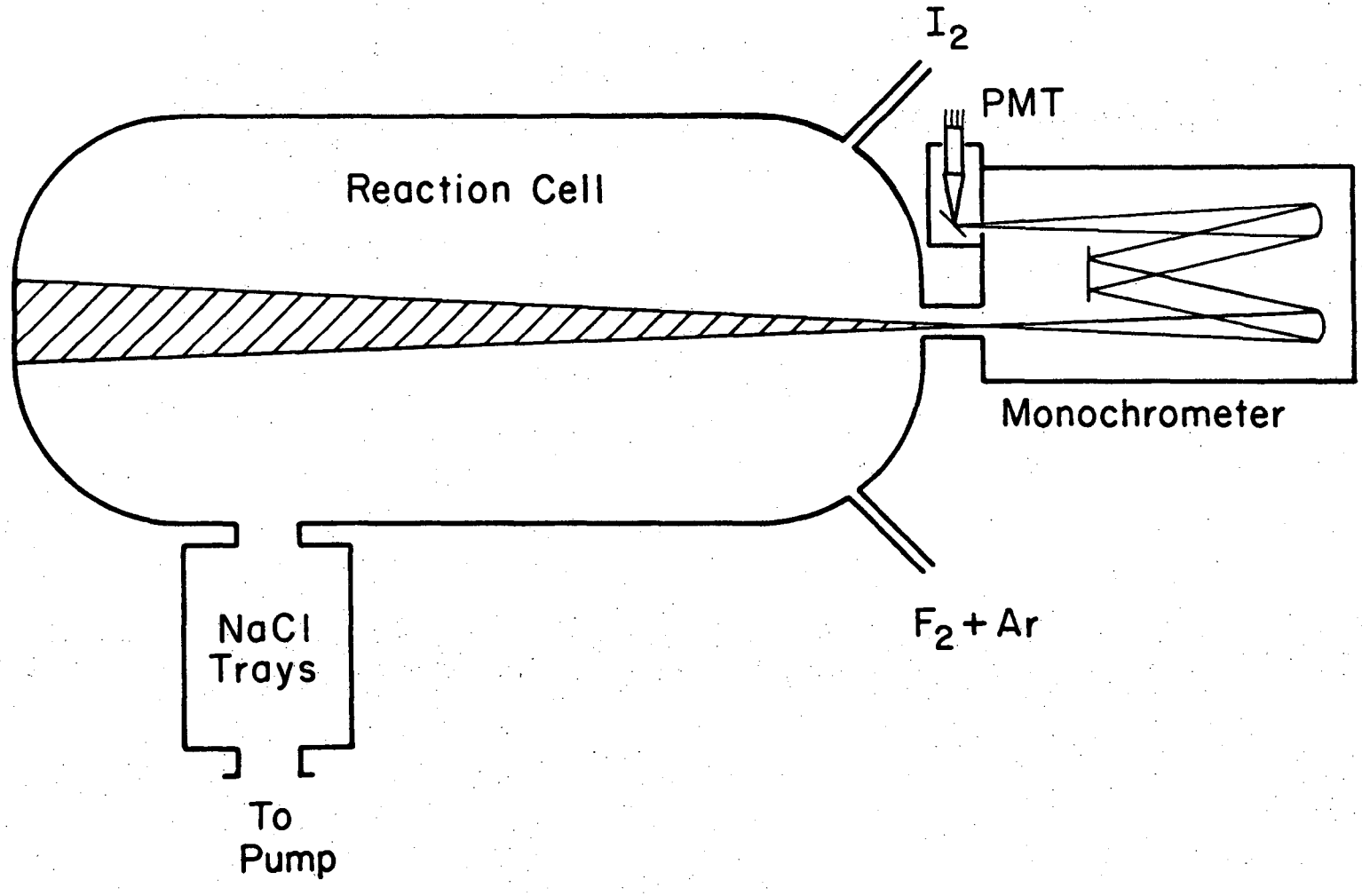

XBL 741-5509

Figure 1

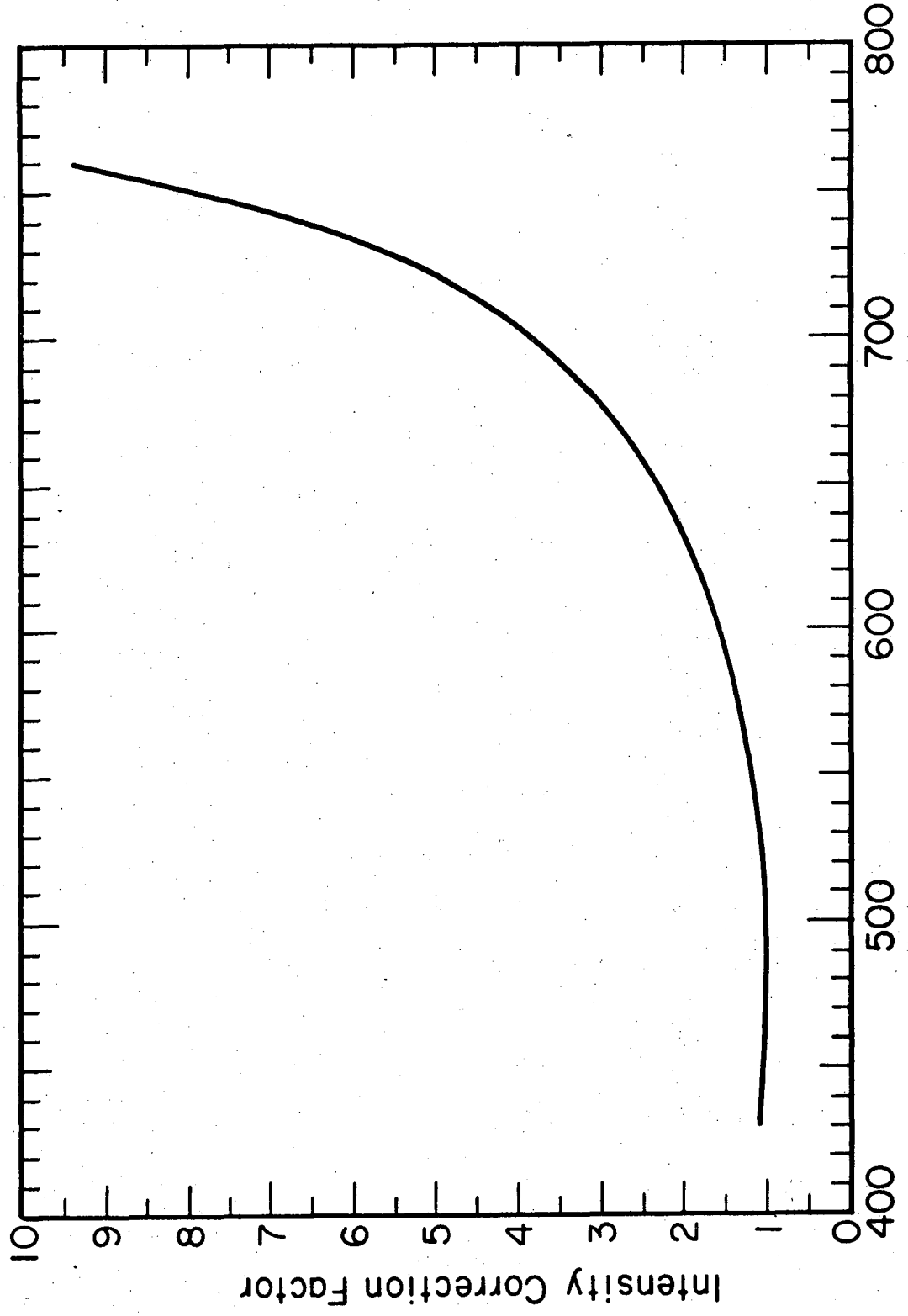

XBL 741-5510

Figure 2

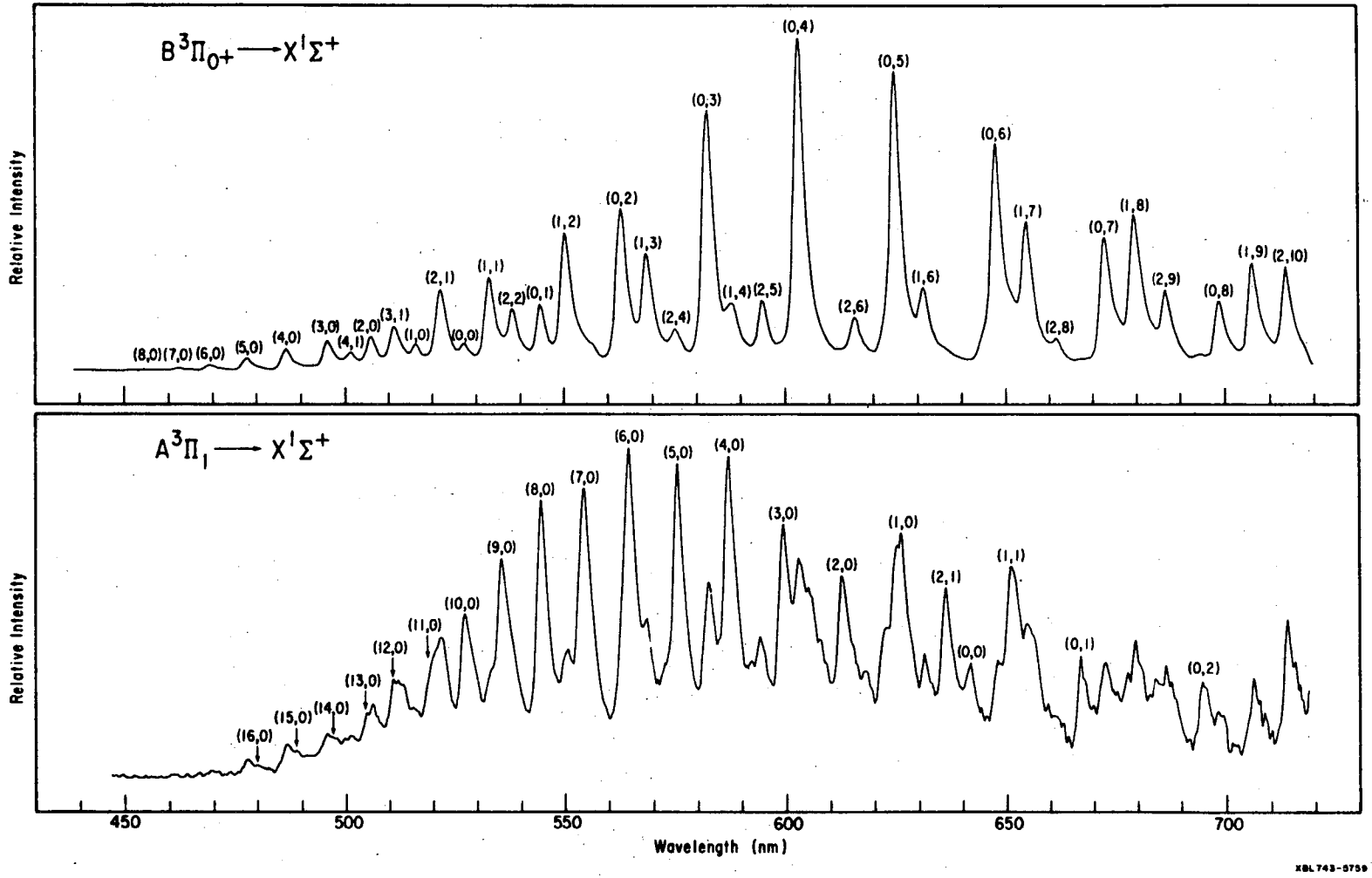
$B^3\Pi_{0^+} \longrightarrow X^1\Sigma^+$
Relative Intensity
(8,0) (7,0) (6,0) (5,0) (4,0) (3,0) (4,1) (2,0) (3,1) (1,0) (2,1) (0,0) (1,1) (2,2) (0,1) (1,2) (0,2) (1,3) (2,4) (0,3) (1,4) (2,5) (0,4) (2,6) (0,5) (1,6) (0,6) (1,7) (2,8) (0,7) (1,8) (2,9) (0,8) (1,9) (2,10)
$A^3\Pi_1 \longrightarrow X^1\Sigma^+$
Relative Intensity
(16,0) (15,0) (14,0) (13,0) (12,0) (11,0) (10,0) (9,0) (8,0) (7,0) (6,0) (5,0) (4,0) (3,0) (2,0) (1,0) (2,1) (0,0) (1,1) (0,1) (0,2)
450 500 550 600 650 700
Wavelength (nm)
XBL 743-5759

Figure 3

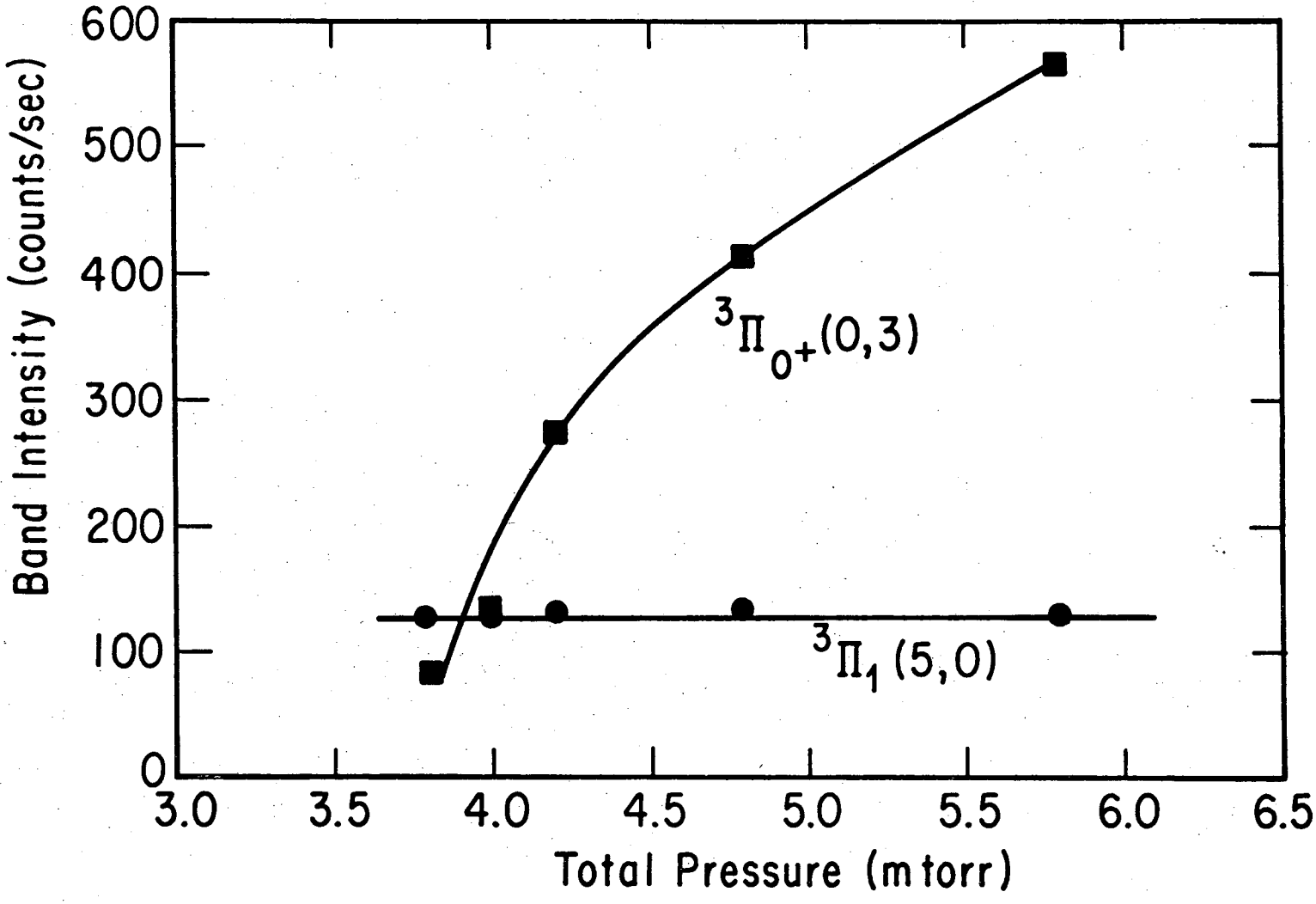

Figure 4

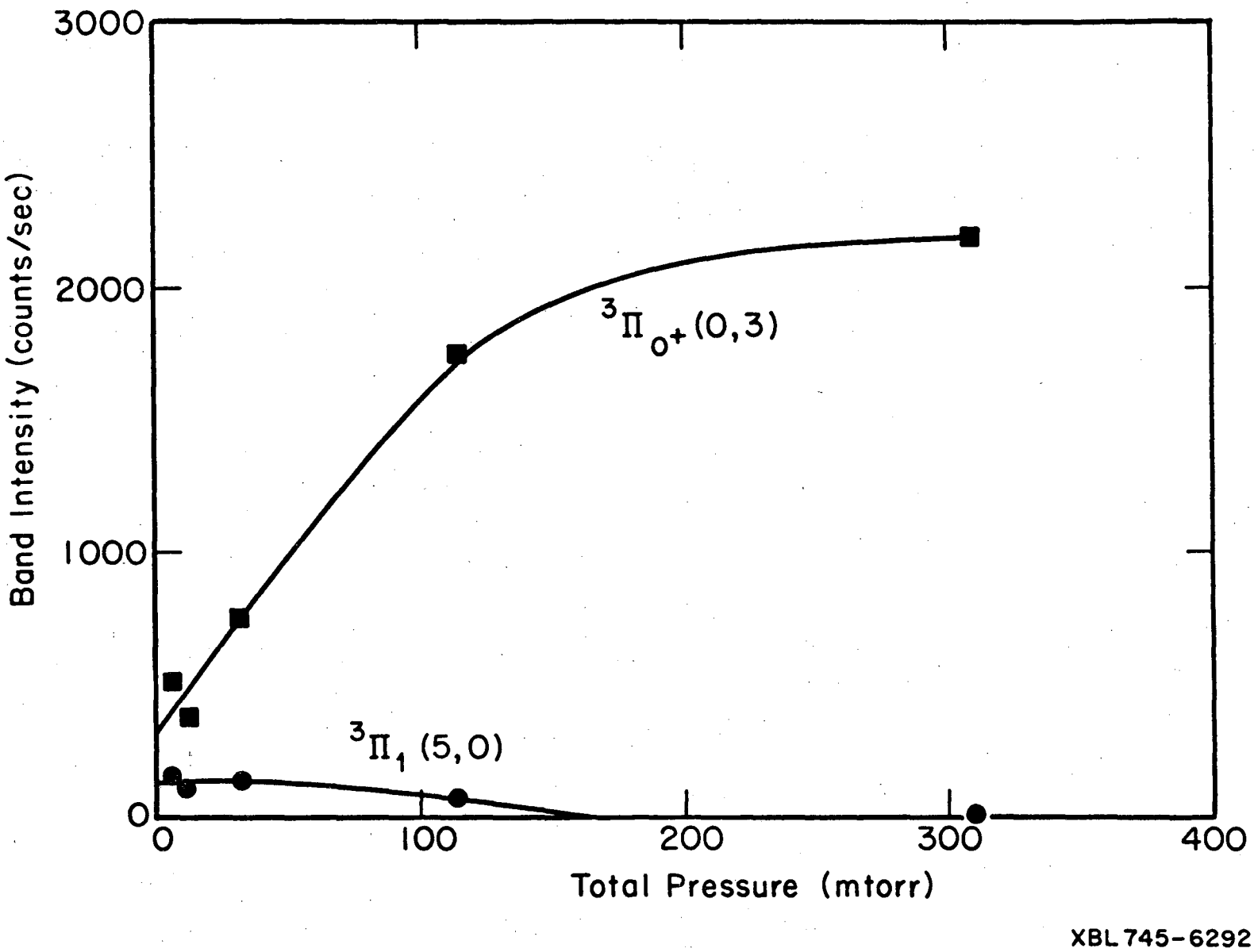
3000
2000
1000
0
Band Intensity (counts/sec)
$^3\Pi_{0^+}(0,3)$
$^3\Pi_1(5,0)$
0
100
200
300
400
Total Pressure (mtorr)
XBL 745-6292

Figure 5a

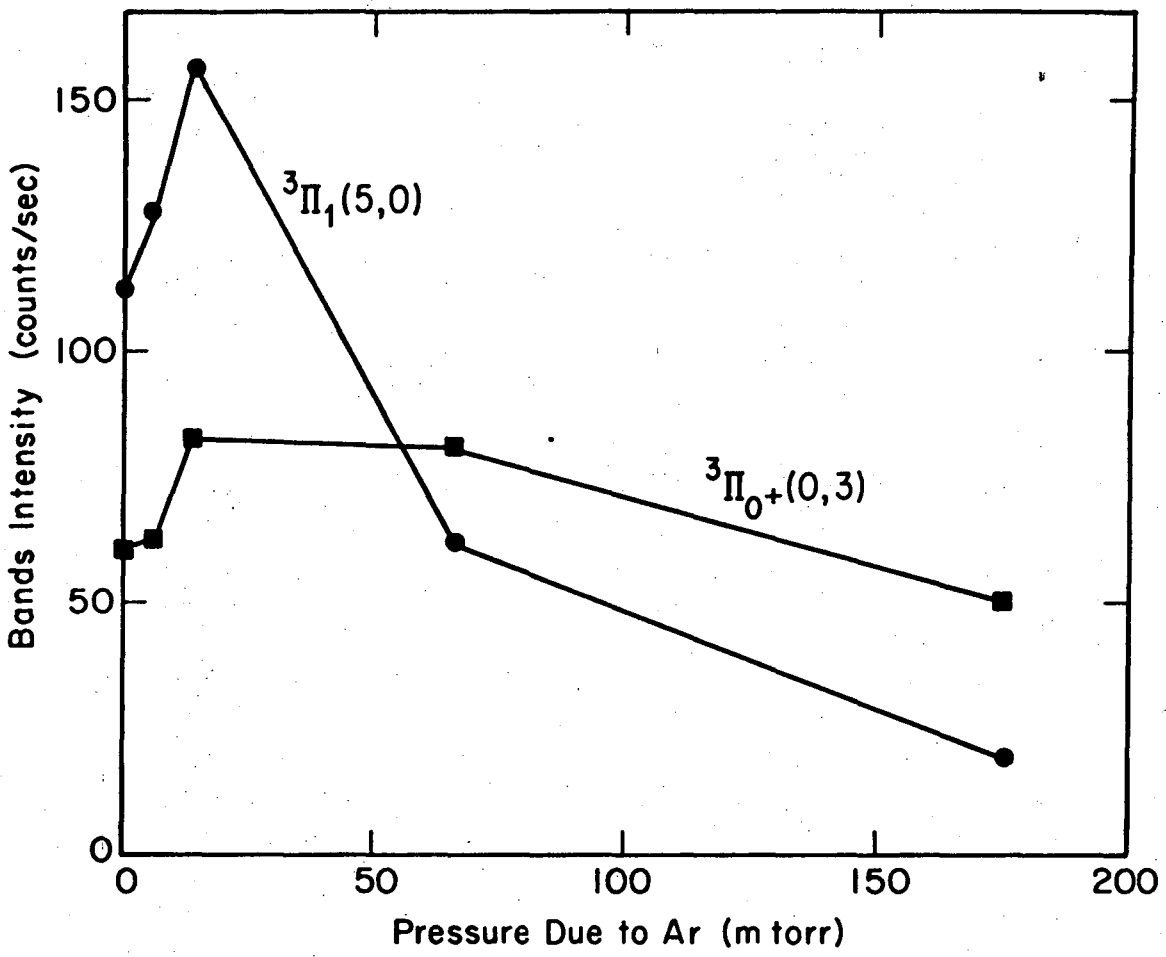

Figure 5b

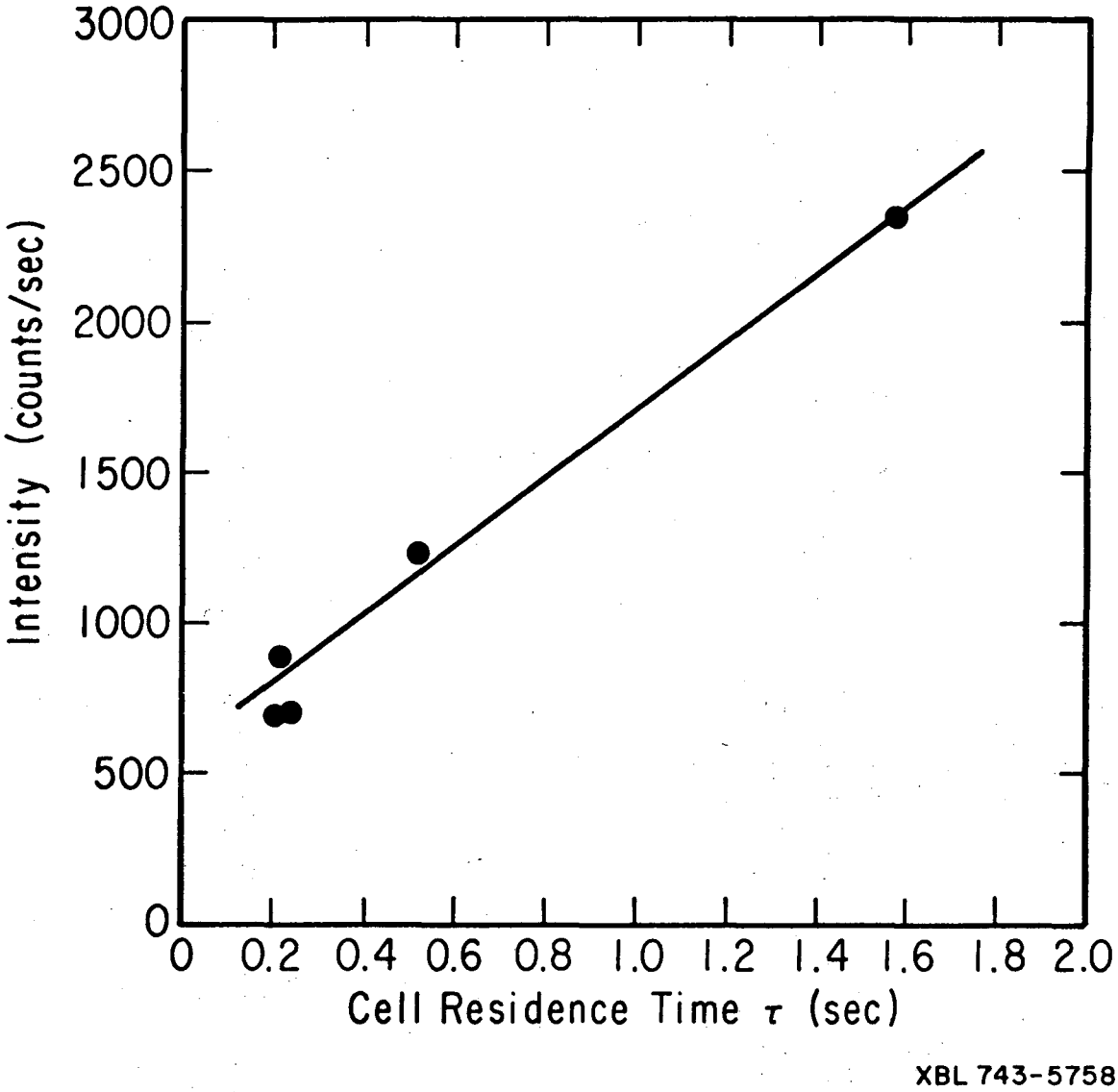
3000
2500
2000
1500
1000
500
0
Intensity (counts/sec)
0
0.2
0.4
0.6
0.8
1.0
1.2
1.4
1.6
1.8
2.0
Cell Residence Time τ (sec)
XBL 743-5758

Figure 6

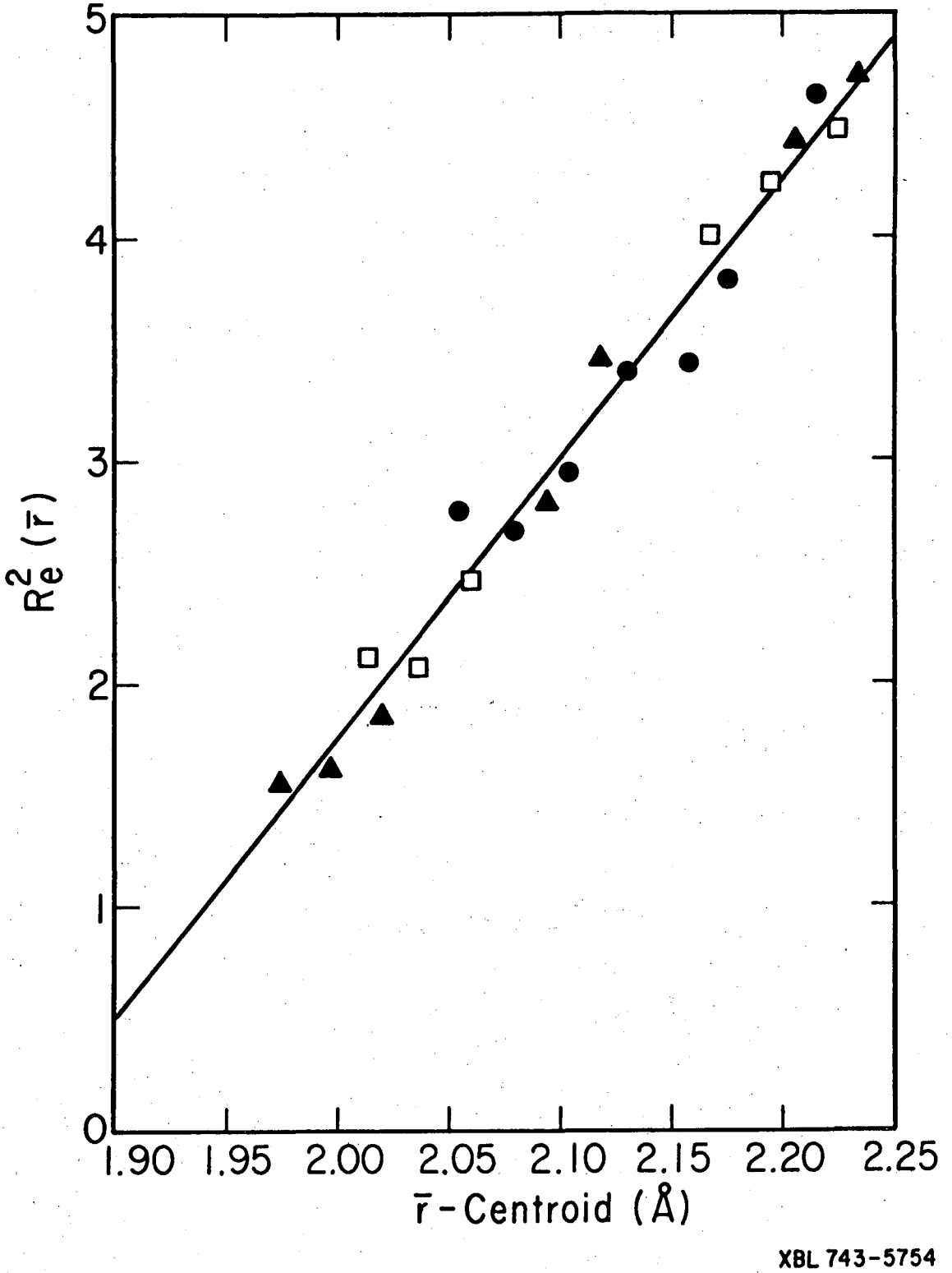

Figure 7

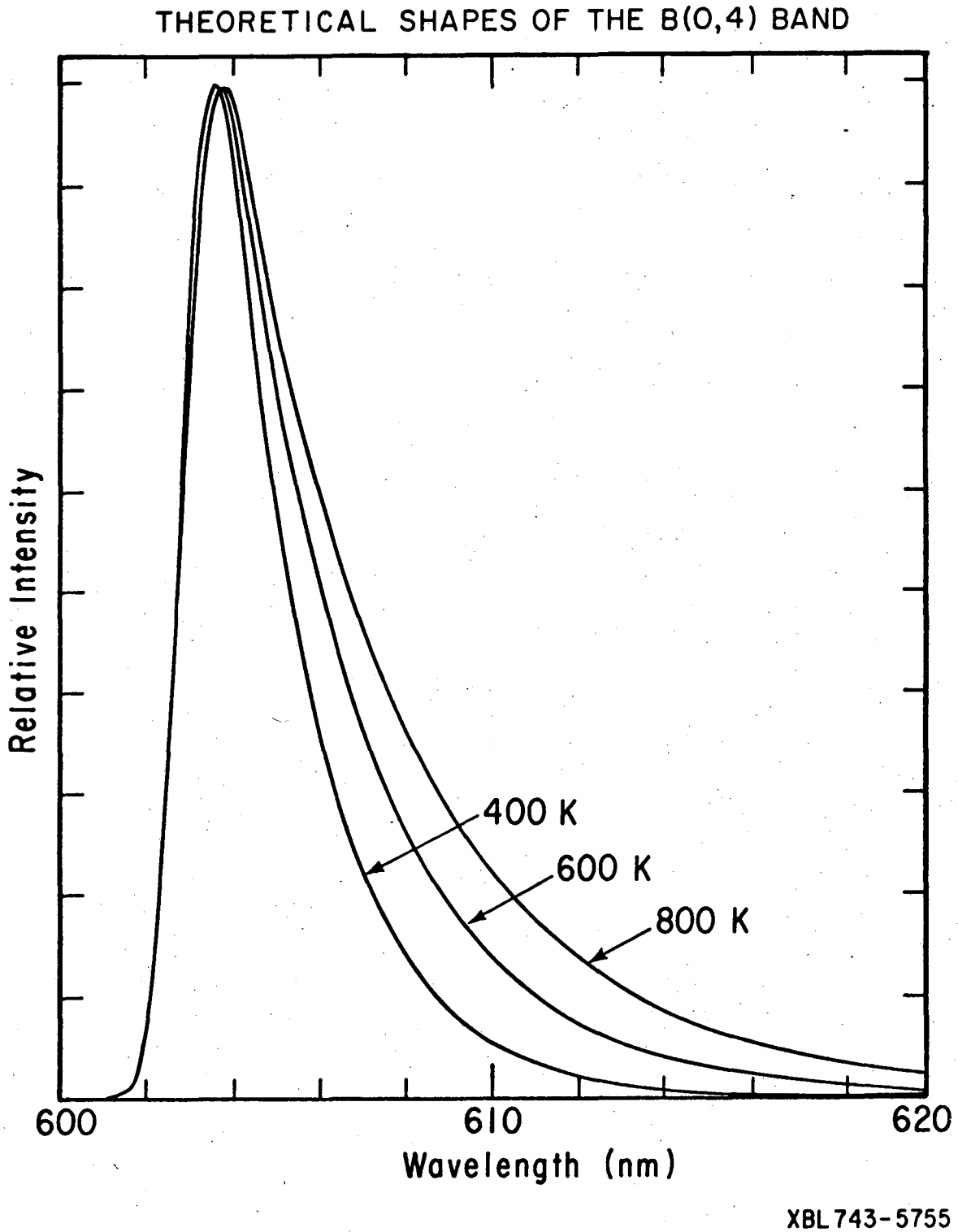
THEORETICAL SHAPES OF THE B(0,4) BAND
Relative Intensity
400 K
600 K
800 K
600
610
620
Wavelength (nm)
XBL743-5755

Figure 8

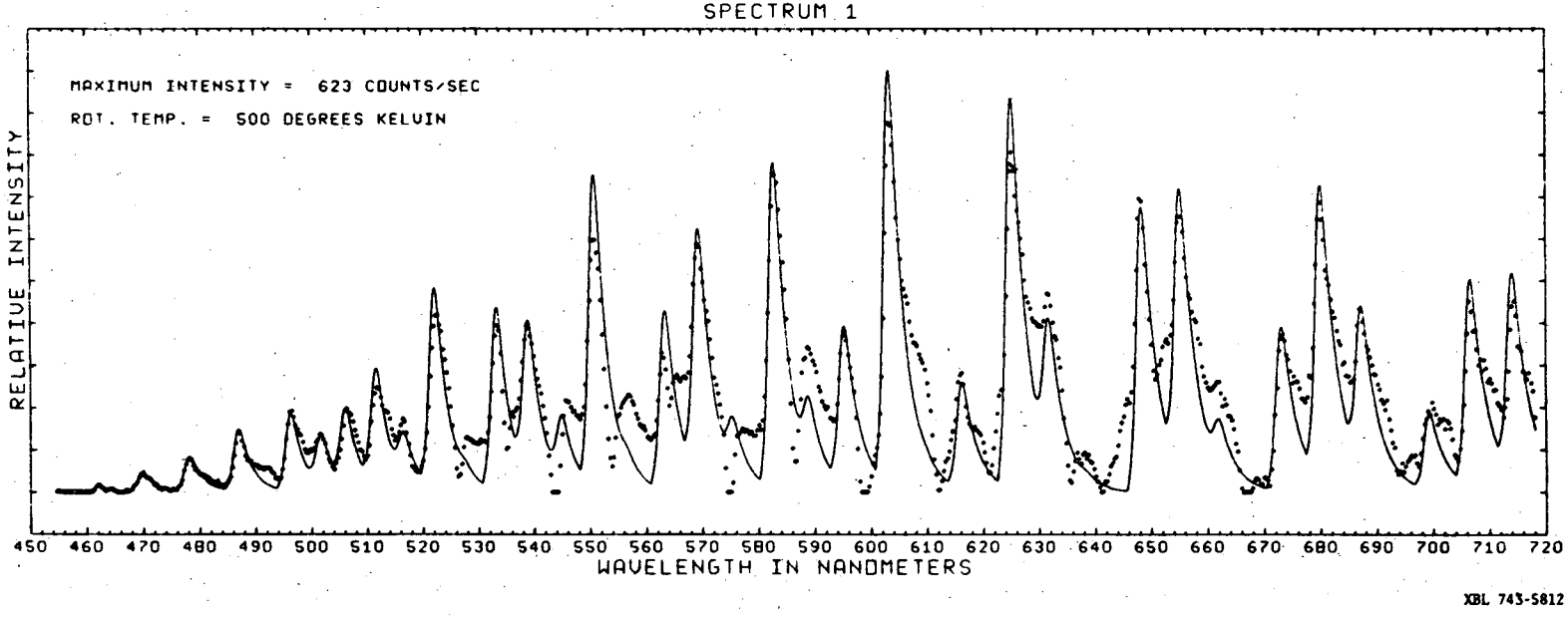

Figure 9a

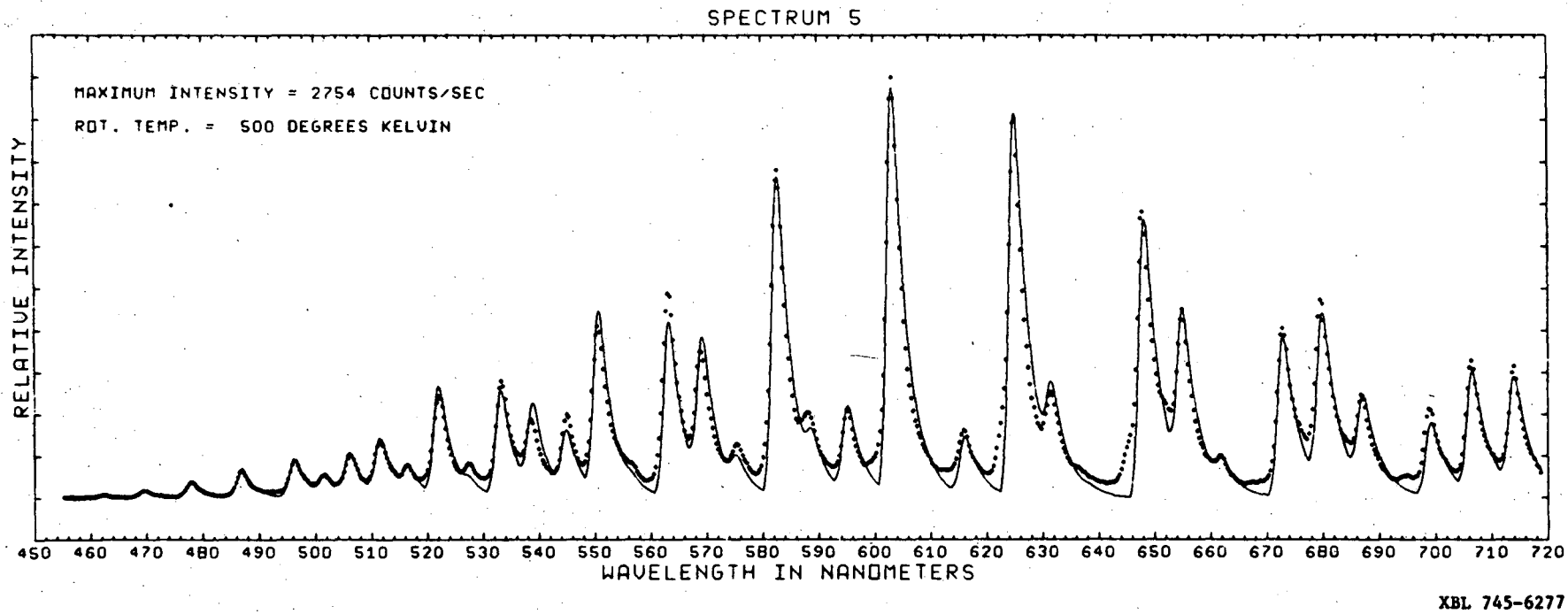
SPECTRUM 5
MAXIMUM INTENSITY = 2754 COUNTS/SEC
ROT. TEMP. = 500 DEGREES KELVIN
RELATIVE INTENSITY
450 460 470 480 490 500 510 520 530 540 550 560 570 580 590 600 610 620 630 640 650 660 670 680 690 700 710 720
WAVELENGTH IN NANOMETERS
XBL 745-6277

Figure 9b

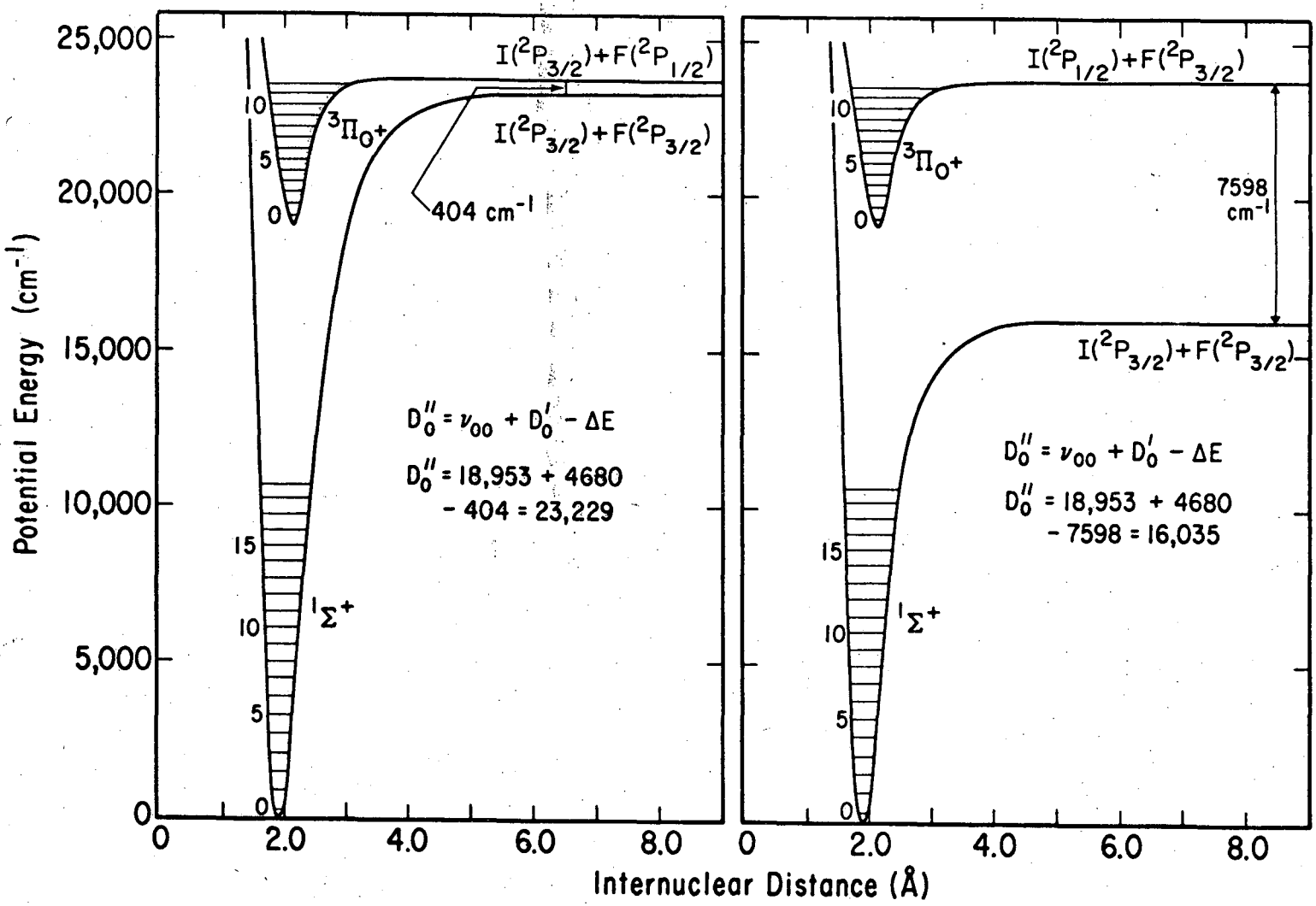

Figure 10

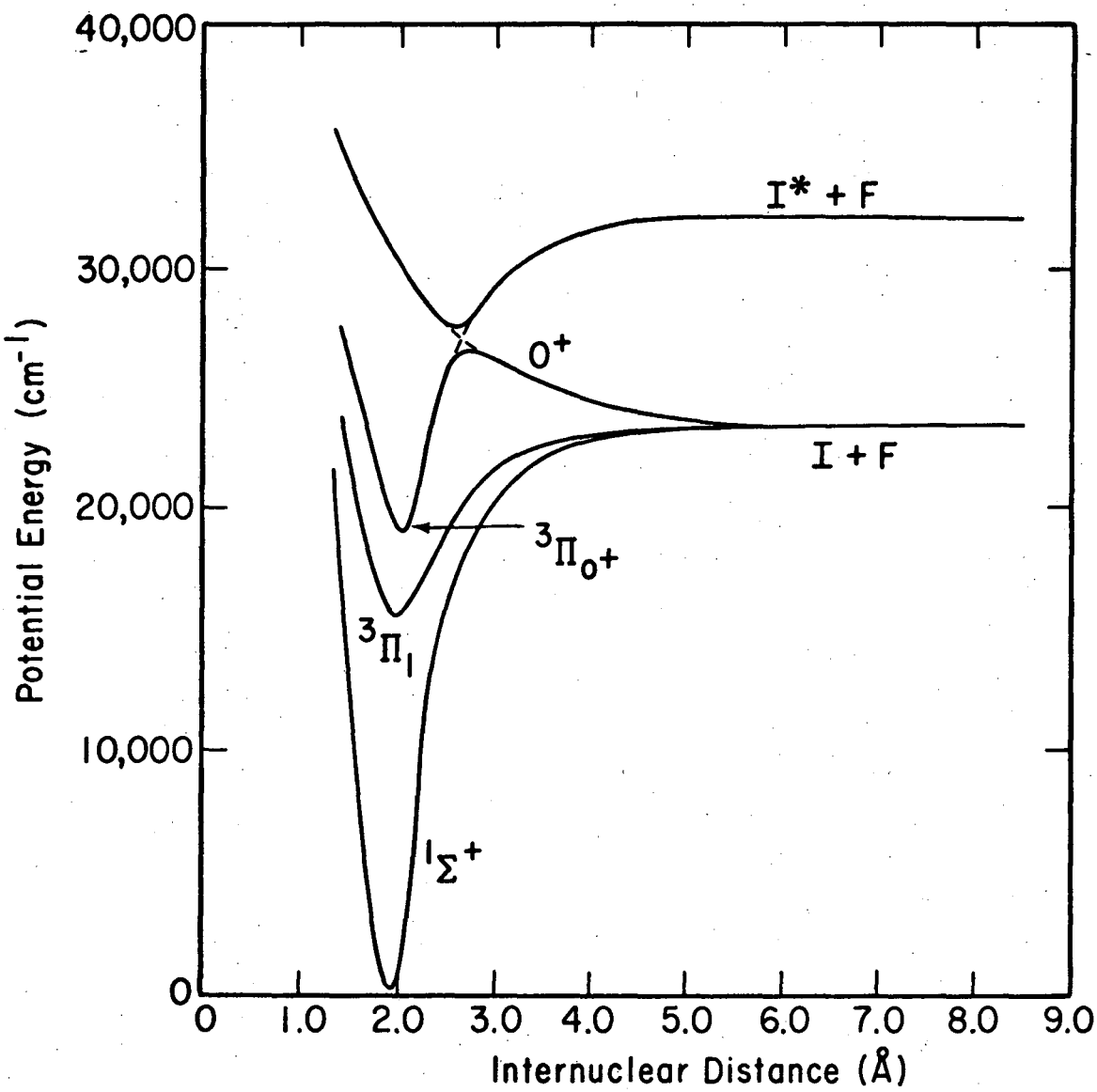

XBL 746-6539

Figure 11a

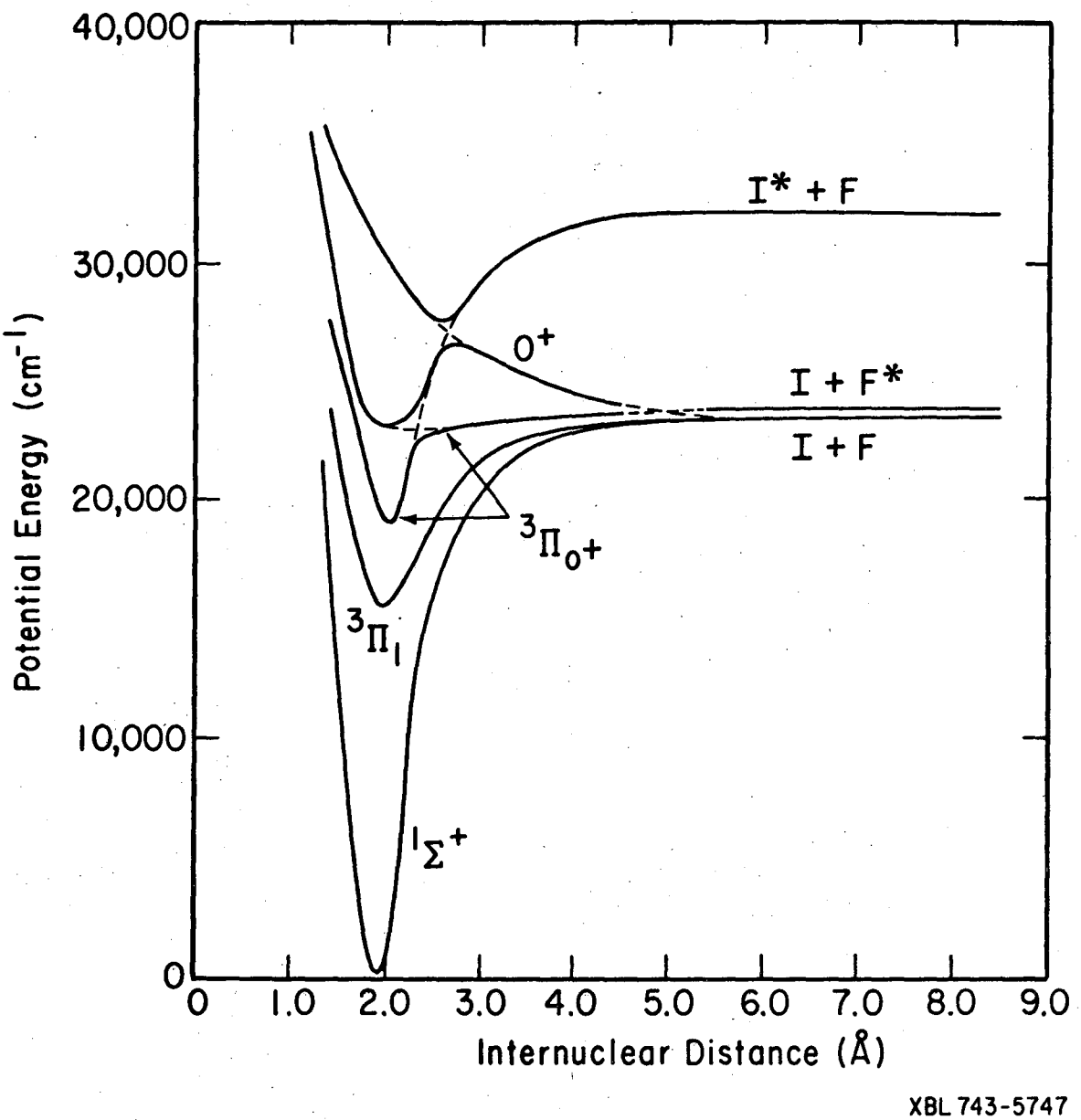

Figure 11b

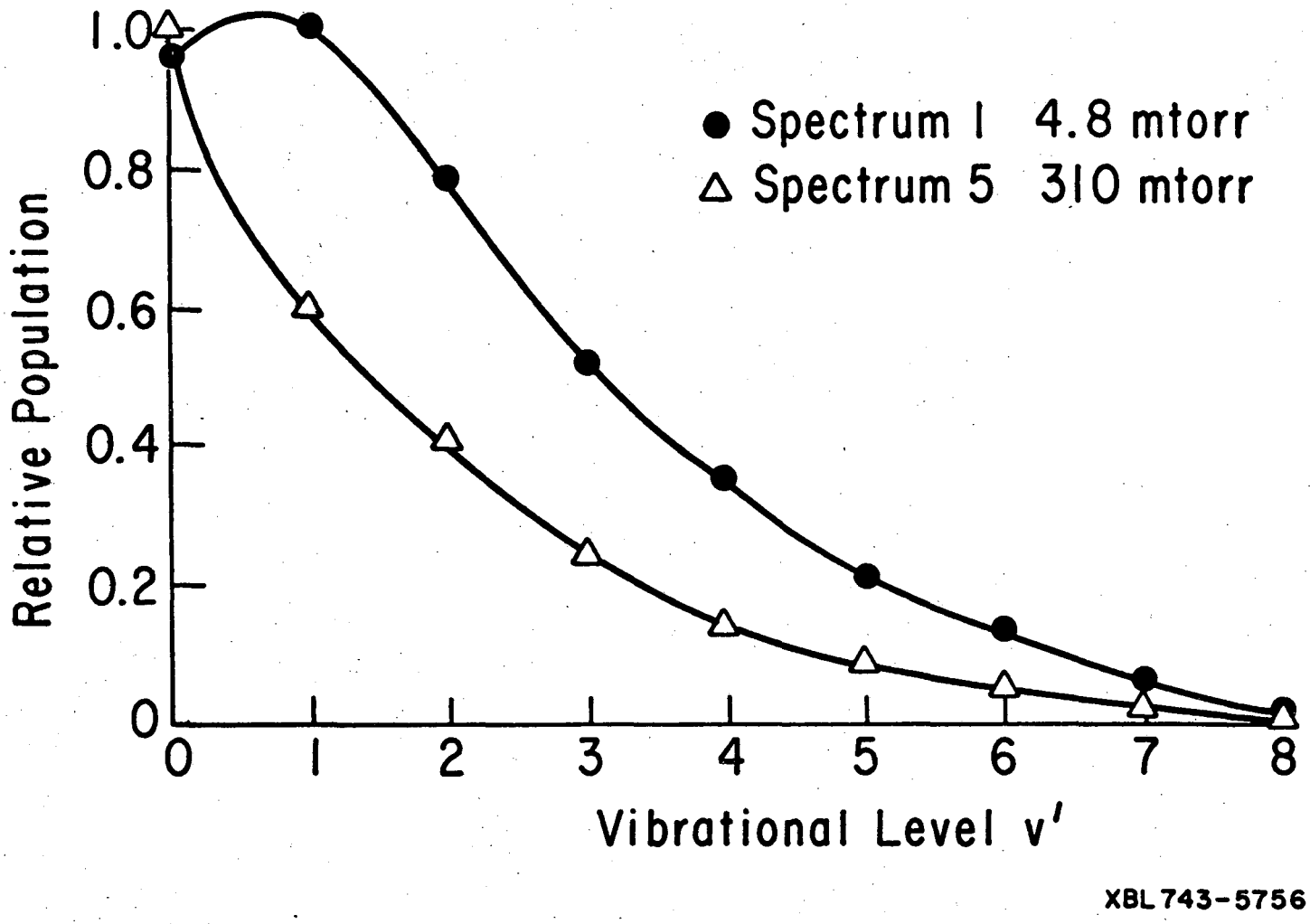
1.0
0.8
0.6
0.4
0.2
0
Relative Population
● Spectrum 1 4.8 mtorr
△ Spectrum 5 310 mtorr
0
1
2
3
4
5
6
7
8
Vibrational Level v'
XBL 743-5756

Figure 12

TECHNICAL INFORMATION DIVISION
LAWRENCE BERKELEY LABORATORY
UNIVERSITY OF CALIFORNIA
BERKELEY, CALIFORNIA 94720